THE UNIVERSITY OF CHICAGO

OPTIMAL LOCKDOWN AND INFORMATION IN A HETEROGENEOUS SIRD MODEL

A BACHELOR THESIS SUBMITTED TO

THE FACULTY OF THE DEPARTMENT OF ECONOMICS

FOR HONORS WITH THE DEGREE OF

BACHELOR OF THE ARTS IN ECONOMICS

BY CHARLES SHI

CHICAGO, ILLINOIS
MAY 2021

Optimal lockdown and information in a heterogeneous SIRD model*

Charles Shi†

May 20, 2021

Abstract

I first investigate the optimal lockdown policy in an economic epidemiological model with heterogeneity in infection, hospitalization, asymptomatic rates and fatality rates. I calibrate parameters based on public health data for the COVID-19 pandemic and find that the information of a social planner greatly influences optimal lockdown policy. I then extend the model to allow the social planner to control the level of testing. Under this framework, I find that a sufficiently low cost of testing allows the social planner to realize a welfare gain by shifting costs of lockdown to costs of testing. However, the optimality of testing is sensitive to initial conditions and demography, suggesting that optimal testing policy also needs to factor in the demographics and state of the pandemic.

Keywords: COVID-19, economic epidemiology, optimal control, heterogeneity, lockdown, social distancing, testing

JEL Codes: C61, I1

*I thank Robert Shimer for advising and providing feedback for this paper. I also thank Victor Lima and Kotaro Yoshida for organizing the undergraduate thesis program.

†University of Chicago, The College

1 Introduction

Epidemiological models for the COVID-19 pandemic have played an important role in policy analysis and have informed both public health officials and the general public. At the time of writing, there are officially 572,000 COVID-19 deaths in the US and 127,000 in the UK[1]. Early models developed by epidemiologists predict 2.2 million deaths in the US (Ferguson et al., 2020) if no actions are taken, and 5,600-120,000 deaths in the UK for various mitigation policies. It is clear that the basic SIRD model with no behavioral responses is not reflective of the pandemic trajectory of virtually any state or nation, implying that policies and/or behavioral responses have successfully altered the trajectory of the pandemic. Yet, the policies that are studied in Ferguson et al. also do not factor in individual incentives. Like many early epidemiological research, the focus of their paper is on the likely outcomes for their policies. What is not examined, however, is the costs and tradeoffs that individuals and governments face in imposing those policies. As a result, it is unclear whether such policies are optimal for welfare, creating a role for economics to play in the wider discourse.

Over the course of the COVID-19 pandemic, economists have synthesized the epidemiological and economic approach to view the pandemic as both a biological and a social problem[2]. The key insight by economists is that individuals in an economy facing the dynamics of a pandemic face a tradeoff: social activity, consumption, production, and the risks and costs of illness and death. Policies that do not factor in endogenous behavioral responses may either overestimate or underestimate the impact of levers that the government may use, such as social distancing, quarantine, vaccine investment, and testing policies.

While the epidemiological angle is undoubtedly important for public health policy, the tremendous costs of the COVID-19 pandemic also come in the form of a prolonged suppression of social activity, leading to the global recession in 2020. In order to better implement policies for future pandemics, both the natural and social effects of this pandemic need to

[1] Based on JHU CSSE COVID-19 data (Dong et al., 2020).

[2] A non-exhaustive list of such research includes: (Farboodi et al., 2020), (Acemoglu et al., 2020), (Alvarez et al., 2020), (Atkeson et al., 2021), (Hall et al., 2020), (Eichenbaum et al., 2020), (Arias et al., 2021)

be examined in tandem.

1.1 Contribution

In this paper I contribute a model that examines how heterogeneity in infection states and age may impact the optimal policy for a benevolent utilitarian social planner that maximizes aggregate welfare. As the COVID-19 disease displays significant heterogeneity across different types of individuals, such as by age, comorbidities, and race, an optimal policy that targets specific groups of individuals may in general significantly outperform non-targeted optimal policies in outcomes such as deaths, welfare, and hospitalization costs. I do so by endogenizing this heterogeneity within the individual's incentives. That is, my model assumes that individuals optimize on social activity and balance their social activity and the risk of infection and death. The social planner will then impose controls on social activity in such a way as to maximize welfare by balancing each individual group's social activity and the externalities they pose towards their own group and others.

By incorporating heterogeneity in the model, I am also able to investigate how the social planner's information affect optimal outcomes and how policies other than lockdown, such as targeted testing, can improve welfare by shifting costs of lockdown to costs of testing. I find that the identification of symptomatic individuals in the population greatly increases welfare in the base calibration. When the social planner cannot differentiate between susceptible, asymptomatic, and symptomatic individuals, however, the welfare is substantially lower. In the model, acquiring information on a substate of infected individuals is equivalent to removing an equality constraint between the level of social activity imposed on susceptible and infected individuals; therefore, optimal welfare is always weakly larger the more information the social planner has.

In particular, testing represents a costly means for the social planner to acquire information on the infection states of individuals. I find that a sufficiently low cost of testing leads to an optimal policy of a targeted testing program that can dramatically limit infections by

giving the social planner clarity on the health statuses of individuals. By doing so the social planner is able to differentiate between uninfected and infected yet asymptomatic/mildly-symptomatic individuals and hence is able to better target her policies. This leads to an increase in welfare as susceptible individuals experience less reduction in social activity as testing increases. For example, the success of Taiwan's national democratized testing and contact tracing program with the aid of crowdsourced technology (Jian et al., (2020)) may be explained partly by a relatively low cost of testing and contact tracing implementation by utilizing a decentralized technological platform. This highlights the potential for governments to invest into a testing and tracing program to lower future testing and tracing costs for the next pandemic.

This model also allows for an examination of how the policy environment may impact the optimal lockdown. In general, different countries and states have different possible levels of enforcement and homophily. A lockdown policy in Tokyo, for example, may not be realistic or optimal in New York due to constraints as inscribed by the law or by public attitude towards the government. Optimal policies in an environment where the young frequently interact with the old and in an environment where the young live in different neighborhoods from the old in general are different. I find that a decrease in the maximum possible lockdown that the social planner can impose leads to a decrease in welfare under optimal policy and a reduction in the advantage from acquiring information.

1.2 Related Literature

Prior to the COVID-19 pandemic there exists research into the synthesis of epidemiological and economic methods. Building on the original SIR model (Kermack and McKendrick), economists have introduced economic considerations (for example: Philipson, Fenichel et al., Toxvaerd). My work is closely related to Fenichel, (2013) and Farboodi et al., (2020) in endogenizing individual and aggregate the utility of social activity as the optimization objective as opposed to minimizing lockdown and costs of deaths and hospitalizations. Doing

so allows the model to capture the pandemic's effects on social activity that may not be completely captured by studying effects on consumption or labor. I follow Farboodi et al. closely as their model shows that laissez-faire and optimal policy outcomes predict an effective reproduction number that stay close to 1, not allowing the pandemic to quickly disappear, which best matches the reality of the COVID-19 pandemic in 2020.

I extend their model to account for heterogeneity broadly following the strategy in Acemoglu et al., (2020). In particular, I examine whether the assumptions about the social planner's information set can be refined to account for the inability or difficulty faced by the social planner in differentiating policy towards asymptomatic and susceptible individuals, following the observation by Farboodi et al.. I also examine whether heterogeneity in infection fatality rates and asymptomatic rates may impact optimal policy. I then extend the model to account for homophily following the discussion of heterogeneity in COVID-19 economic models in Ellison, (2020) in order to capture heterogeneity in contacts following a class of literature such as Stock, (2020). However, relative to the literature on heterogeneous COVID-19 economic models, I focus on understanding behavioral responses and welfare measures derived from social activity rather than optimizing on the costs of lockdown and deaths.

My paper is also related to the literature on the economic impacts of testing and contact tracing. Much of the literature in this area, such as Ayres et al., (2020), has focused on the network effects of contact tracing. For example, Almagor and Picascia, (2020) uses an agent-based model to assess the efficacy of testing and contact tracing. However, relative to these papers I model testing as another policy lever that the social planner may employ and consider the trade-off facing her. As testing is imperfect and costly, it is not in general true that these policies will result in higher welfare in the economy.

The rest of the paper is organized as follows: In Section 2 I motivate and develop the epidemiological and economic components of the basic model. I then characterize the social planner's problem and discuss important optimal conditions that grant insight into the social

planner's problem. Then, to exploit the advantages of heterogeneity, I extend the basic model to consider testing, homophily, and imperfect enforcement. In Section 3 I start by calibrating the basic model and discuss the assumptions and methods used for the calibration of key parameters. Then, I examine the impact of the social planner's information set on the trajectory of the pandemic, the optimal lockdown policy, and hospitalizations and deaths. I then discuss the numerical results for the model extended with testing, homophily, and imperfect enforcement. In Section 4 I situate findings of my model within data from the COVID-19 pandemic. In Section 5 I discuss the findings and limitations. In the Appendix I detail the computational method.

2 Model

In this section, I develop an economic epidemiological model that combines features from Farboodi et al. and Acemoglu et al.. Specifically, I assume that agents in the economy display heterogeneity in infection fatality rate, hospitalization rate, and optimize on their social activity. Deaths and hospitalizations are costly in this economy. I follow Acemoglu et al. and examine how heterogeneity can impact public health and welfare outcomes through policies such as testing and targeted policies. However, I also follow Farboodi et al. and let the social planner optimize the welfare of individuals directly in order to endogenize behavioral responses.

2.1 Setup

2.1.1 Epidemiological Framework

The epidemiological block of the model is an SIRD model with multiple infection states. Individuals are always in exactly one health state: susceptible (S), infected (I), recovered (R), or dead (D). I subdivide the infected state into three different states. Infected individuals may either be asymptomatic (I_A), symptomatic (I_S), or hospitalized (I_H). Individuals may

only transfer between health states as follows (see also Figure 1): Susceptible individuals can only transfer into one of the three infected states. Infected individuals can transfer into either the recovered or dead states. Finally, recovered and dead individuals do not transfer into any other state, meaning that we assume recovery from the COVID-19 virus confers permanent immunity. This framework also implies that infected individuals may not change between the infection states, which makes this model different from an SEIRD model which emphasizes the transition from an asymptomatic and exposed state (E) to an infected state. I do so to limit the complexity of the model and to focus on studying the effects of heterogeneity in infection states[3].

The model assumes heterogeneity in the population. Each individual is categorized as a type-j individual, where their type influences the probability of transferring between different health states. For example, a type-y individual may be categorized as young and have a 0.01 probability of transferring from S to I_H, while a type-o individual may be categorized as old and have a 0.1 probability of transferring from S to I_H. I calibrate these parameters more formally in Section 3.1.

2.1.2 Epidemiological Dynamics

Let S, I, R, D denote the proportion of the population in each corresponding health state. Let the subscript denote the subdivided health state and the superscript denote the individual type in each corresponding health state. For example, I_S^3 denotes the proportion of type-3 individuals that are infected and symptomatic within the general population.

[3]The COVID-19 pandemic affects the population in a highly heterogeneous way: while many individuals fall sick and even die, some may not even be aware that they are carriers of the virus and infectious, displaying no symptoms. As a result of this heterogeneity, the behaviors of individuals by infection states may not in general be equal.

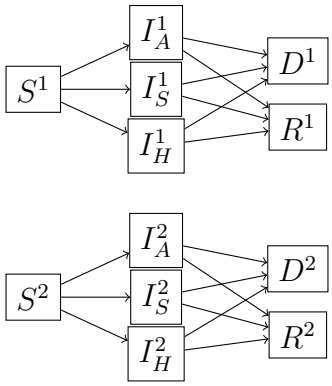

Figure 1
Flowchart between health states for an
economy with 2 types of individuals

The dynamics of the epidemiological block then follows the system of ODEs as follows:

$$\begin{aligned}
\dot{S^j} &= -\beta S^j \sum_{k,h} \sigma_h^{j,k} C_h^{j,k}(\cdot) I_h^k, \\
\dot{I_h^j} &= \beta \tau_h^j S^j \sum_{k,h} \sigma_h^{j,k} C_h^{j,k}(\cdot) I_h^k - \gamma_h^j I_h^j, \\
\dot{R^j} &= \sum_h \left(1 - \pi_h^j\right) \gamma_h^j I_h^j, \\
\dot{D^j} &= \sum_h \pi_h^j \gamma_h^j I_h^j,
\end{aligned} \tag{1}$$

where β is the base infection doubling rate for a type j individual, γ_h^j is the recovery rate for a type j individual in infection state I_h^j, π_h^j is the death rate for a type j individual in infection state I_h^j, $\sigma_h^{j,k}$ describes the level of association/homophily between individual types, and $C_h^{j,k}(\cdot)$ is the contact function between a susceptible individual of type j and an infected individual of type h in infection sub-state h and take their activity levels as inputs. Furthermore,

$$I^j \equiv \sum_h \tau_h^j I_h^j$$

where τ_h^j is the likelihood for a type j individual to transition into an infection state I_h upon infection.

2.1.3 Individual Preferences and Social Activity

Individuals optimize on one object across different health states: social activity. Each individual of type j gains utility from social activity by the utility function $u^j(a_H, H)$, where their utility for social activity may change depending on their health state. I assume that there is a bliss point for u conditional on a health state H. Denote a_H^{j*} as the activity bliss point that maximizes the type j individual's utility conditional on their health state being H. In general we may expect $a_{H_1}^{j*} \neq a_{H_2}^{j*}$ for different health states H_1, H_2. For example, a hospitalized individual may not wish to pursue social activity at a level as high as they would were they recovered because they wish to rest, so that even if they were given the opportunity to do so, they will still optimize at $a < a_R^*$. Formally, following Farboodi et al. I set the utility representation to $u^j(a_H, H) = \log a_H - a_H + a_H^{j*}$, where $a_H^{j*} = 1$ for susceptible and recovered individuals. I assume asymptomatic and symptomatic individuals are well enough to wish to engage in the same level of social activity as susceptible and recovered individuals. Hospitalized individuals, on the the other hand, may desire to partake in less social activity even when there is zero altruism, because they may be too sick or lethargic.

Social activity in this model is a representative activity that individuals partake in that may lead to virus transmission and can be interpreted as an average of risky (in the context of COVID-19) activities one may pursue, such as going to the gym, social gatherings and parties, and purchasing groceries. As such, increasing social activity reflects increasing contacts with other individuals.

2.1.4 Contact Function and Homophily

To endogenize behavioral responses and their influence on the dynamics of the pandemic, let $C_h^{j,k}\left(a_S^j, a_{I_h}^k\right)$ be the contact function between a susceptible individual of type j and an infected individual of type h in infection sub-state h. Note that if $C_h^{j,k}(\cdot) = 1$ for all j, k, h then the system of ODEs in Equations 1 becomes that of the basic SIRD model, i.e., a lack of behavioral responses to the pandemic. Additionally, I model homophily as in general we

may expect that individuals of each type j tend to associate and bond with individuals of their same type. For example, a young person may tend to live in a younger neighborhood and as such their activities may predominantly be with young people. In this sense, we should expect that C^j would be impacted a unit of deviation in a_I^j more than that by a unit of deviation in a_I^{-j}. That is, an older infected individual increasing or reducing their activity by a unit will impact the contact function of a young person less than that which occurs when a young infected individual increased or reduced their activity by that same unit.

I follow Farboodi et al. and utilize a quadratic matching technology for the contact function. That is,

$$C_h^{j,k}\left(a_S^j, a_{I_h}^k\right) = a_S^j a_{I_h}^k. \tag{2}$$

I implicitly assume random search here. That is, conditional on a type j individual contacting a type k individual with infection status I_h, the type j individual contacts randomly between all such individuals. I assume that contacts have minute impact on recovery or death, so that the contact function does not appear in $\dot{R}$ and $\dot{D}$. The quadratic matching assumption reflects the airborne and density-dependence nature of COVID-19. The medical literature suggests that density-dependent transmission better reflects directly transmitted diseases (Smith et al., (2009)), for which a quadratic matching technology is better suited for[4].

[4]See also dinoverm and McCallum et al. for a discussion on various approaches to modeling contacts. However, in the absence of more rigorous data that will illuminate what transmission function is most appropriate for COVID-19, I follow many others and assume quadratic matching as the airborne and directly transmitted nature of COVID-19 seems to best correspond to pathogens that have traditionally been modeled with density-dependent transmission functions, such as the flu.

I model homophily with the parameter σ[5]. For each j, I require that

$$\sum_k \sigma^{j,k} = |\{k\}|$$

so that in the homogeneous case with $C^{j,k} = 1$ and $I^k = \bar{I}$ for all j, k, the model corresponds to the standard SIRD model. However, I relax this requirement for hospitalization as it is expected that hospitalized individuals only contact healthcare providers and relatives and friends to a lesser extent while they're in the hospitalization state. In general we may expect $\sigma^{j,j} > \sigma^{j,k}$ whenever $k \neq j$. Furthermore, for non-hospitalized individuals I impose the restriction that

$$\sigma^{j,k} = \sigma^{k,j}$$

so that homophily is symmetric.

I note that my use of the contact function and homophily model different facets of the pandemic. The contact function models endogenous effects of individuals' behavioral responses on their likelihood of getting infected. For example, if symptomatic individuals are altruistic and are concerned with the externalities they cause, they will lower their activity level, therefore decreasing the infection rate of all people in contact with these symptomatic individuals. In contrast, homophily models exogenous aspects of the pandemic that the individual cannot control. For example, older people may be homophilic by virtue of living within a neighborhood that tends to be old, and so contact older people more frequently.

[5]Ellison, (2020) discusses one method of modeling homophily, using

$$\beta_{ij}^h = \begin{cases} \gamma R_{0i} \left(h + (1-h) \frac{R_{0j}}{\sum_k R_{0k}} \right) & \text{if} j \neq i, \\ \gamma R_{0i} (1-h) \frac{R_{0j}}{\sum_k R_{0k}} & \text{if} j \neq i. \end{cases}$$

This has the advantage of allowing the parameter h to fully control the level of homophily within each group, but will greatly increase the complexity of the current model setup. I instead opted to follow Acemoglu et al. and use a homophily matrix, which I will discuss in Section 3.7.

2.2 Social Optimum

2.2.1 Social Planner's Problem

I set up the problem faced by a benevolent utilitarian social planner facing the state variables S, I, R, D for each individual type and each infection sub-state and is able to control the social activity of individuals. Critically, in the absence of testing and contact tracing, the social planner is unable to differentiate between susceptible and infectious yet asymptomatic individuals and hence can only control $a_S^j, a_{I_S}^j, a_{I_H}^j$, and a_R^j for each individual type j, with the constraint that $a_S^j = a_{I_A}^j$. The ability for the social planner to directly control the social activity of symptomatic-infected individuals reflects an idealized world wherein individuals upon discovering their symptoms immediately act according to governmental health guidelines [6]. Individuals discount the future at a constant rate ρ and expect a perfect and immediate cure to arrive in a Poisson process and further discount the future at a constant rate δ [7]. The social planner also internalizes the cost of infections with the parameters $\kappa_A^j, \kappa_S^j, \kappa_H^j$ and ψ, describing the expected cost of death in infection states I_A, I_S, I_H for a type j individual and the expected cost of hospitalization ψ for all individuals, which I assume are identical (that is, conditional on hospitalization individuals of all types require the same level of medical attention and resources).

Denote $\mathcal{J}$ as the set of individual types. For instance, $\mathcal{J} = \{y, m, o\}$ describes an economy with young, middle-aged, and old individual types. The planner then solves

$$\max_{\left\{a_S^j, a_{I_S}^j, a_{I_H}^j, a_R^j\right\}_{j\in\mathcal{J}}} \int_0^\infty e^{-(\rho+\delta)t} \sum_j \Big[S^j u^j\left(a_S^j, S\right) + I_A^j u^j\left(a_S^j, I_A\right) + I_S^j u^j\left(a_{I_S}^j, I_S\right) + I_H^j u^j\left(a_{I_H}^j, I_H\right) + R^j u^j\left(a_R^j, R\right) - \sum_h \left(\gamma_h^j I_h^j\left(\kappa_h^j + \psi_h\right)\right)\Big] \, dt \tag{3}$$

[6] I will also explore the social optimum for different information sets in Section 3. For example, a social planner who can only impose social activity restrictions on hospitalized-infected individuals solve nearly the same problem as in Equation 4, except the set of controls is limited to $\left\{a_S^j, a_{I_H}^j\right\}_{j\in\mathcal{J}}$.

[7] Qualitative features of the model where the vaccine arrives exactly at some time T are similar, except that social activity converges to 1 as $t \to T$.

subject to Equations 1 and where $\psi_A = \psi_S = 0$. Note that given the quadratic matching technology, the social activity of recovered individuals does not impact $\dot{I}$ and cause no externality; therefore it is optimal to set a_R^j to 1. As such we can reduce Equation 3 to

$$\max_{\left\{a_S^j, a_{I_S}^j, a_{I_H}^j\right\}_{j\in\mathcal{J}}} \int_0^\infty e^{-(\rho+\delta)t} \sum_j \Big[S^j u^j\left(a_S^j, S\right) + I_A^j u^j\left(a_S^j, I_A\right) + I_S^j u^j\left(a_{I_S}^j, I_S\right) + I_H^j u^j\left(a_{I_H}^j, I_H\right) - \sum_h \left(\gamma_h^j I_h^j\left(\kappa_h^j + \psi_h\right)\right) \Big] \, dt \tag{4}$$

2.2.2 Optimality Conditions

Then, note that the current value Hamiltonian is

$$\begin{aligned} \mathcal{H} = e^{(\rho+\delta)t} \sum_j \Big[& S^j u^j\left(a_S^j, S\right) + I_A^j u^j\left(a_S^j, I_A\right) + I_S^j u^j\left(a_{I_S}^j, I_S\right) + I_H^j u^j\left(a_{I_H}^j, I_H\right) \\ & - \sum_h \left(\gamma_h^j I_h^j\left(\kappa_h^j + \psi_h\right)\right) \\ & - \lambda_S^j \beta S^j \sum_{k,h} \sigma_h^{j,k} C_h^{j,k}\left(\cdot\right) I_h^k + \sum_h \left(\lambda_{I_h}^j \left(\beta \tau_h^j S^j \sum_{k,h} \sigma_h^{j,k} C_h^{j,k}\left(\cdot\right) I_h^k - \gamma_h^j I_h^j\right)\right) \Big] \end{aligned} \tag{5}$$

where λ_H^j denotes the co-state variable associated with the corresponding constraint $\dot{H}^j = g\left(\cdot\right)$ describing the dynamics for individuals in health state H and type j. The first necessary condition is that the vector of optimal controls maximize the current-value Hamiltonian, so that

$$\left(a_S^{j*}, a_{I_S}^{j*}, a_{I_H}^{j*}\right) = \underset{\left(a_S^j, a_{I_S}^j, a_{I_H}^j\right)}{\arg\max} \; \mathcal{H}.$$

Hence, for each j,

$$\begin{aligned}
&S^j \frac{\partial u^j\left(a_S^{j*}, S\right)}{\partial a_S^j} + I_A^j \frac{\partial u^j\left(a_S^{j*}, I_A\right)}{\partial a_S^j} - \lambda_S^j \beta S^j \sum_{k,h}\left(\sigma_h^{j,k} \frac{\partial C_h^{j,k}\left(a_S^{j*}, \cdot\right)}{\partial a_S^j} I_h^k\right) \\
&+ \lambda_{I_A}^j \beta \tau_A^j S^j \sum_{k,h}\left(\sigma_h^{j,k} \frac{\partial C_h^{j,k}\left(a_S^{j*}, \cdot\right)}{\partial a_S^j} I_h^k\right) - \sum_{k\neq j}\left(\lambda_S^k \beta S^k \sigma_A^{k,j} \frac{\partial C_A^{k,j}\left(\cdot, a_S^{j*}\right)}{\partial a_S^j} I_A^j\right) \\
&+ \sum_{k\neq j}\sum_{h}\left(\lambda_{I_h}^k \beta \tau_h^k S^k \sigma_A^{k,j} \frac{\partial C_A^{k,j}\left(\cdot, a_S^{j*}\right)}{\partial a_S^j} I_A^j\right) = 0
\end{aligned} \tag{6}$$

$$\begin{aligned}
&I_S^j \frac{\partial u^j\left(a_{I_S}^{j*}, I_S\right)}{\partial a_{I_S}^j} + \lambda_{I_S}^j \beta \tau_S^j S^j \sum_{k,h}\left(\sigma_h^{j,k} \frac{\partial C_h^{j,k}\left(a_{I_S}^{j*}, \cdot\right)}{\partial a_{I_S}^j} I_h^k\right) \\
&- \sum_{k\neq j}\left(\lambda_S^k \beta S^k \sigma_S^{k,j} \frac{\partial C_S^{k,j}\left(\cdot, a_{I_S}^{j*}\right)}{\partial a_{I_S}^j} I_S^j\right) + \sum_{k\neq j}\sum_{h}\left(\lambda_{I_h}^k \beta \tau_h^k S^k \sigma_S^{k,j} \frac{\partial C_S^{k,j}\left(\cdot, a_{I_S}^{j*}\right)}{\partial a_{I_S}^j} I_S^j\right) = 0
\end{aligned} \tag{7}$$

$$\begin{aligned}
&I_H^j \frac{\partial u^j\left(a_{I_H}^{j*}, I_H\right)}{\partial a_{I_H}^j} + \lambda_{I_H}^j \beta \tau_H^j S^j \sum_{k,h}\left(\sigma_h^{j,k} \frac{\partial C_h^{j,k}\left(a_{I_H}^{j*}, \cdot\right)}{\partial a_{I_H}^j} I_h^k\right) \\
&- \sum_{k\neq j}\left(\lambda_H^k \beta S^k \sigma_H^{k,j} \frac{\partial C_H^{k,j}\left(\cdot, a_{I_H}^{j*}\right)}{\partial a_{I_H}^j} I_H^j\right) + \sum_{k\neq j}\sum_{h}\left(\lambda_{I_h}^k \beta \tau_h^k S^k \sigma_H^{k,j} \frac{\partial C_H^{k,j}\left(\cdot, a_{I_H}^{j*}\right)}{\partial a_{I_H}^j} I_H^j\right) = 0
\end{aligned} \tag{8}$$

The second necessary condition is that the optimal dynamics for the state is such that

$$\dot{H}^{j*} = \frac{\partial \mathcal{H}}{\partial \lambda_H^j}$$

Hence, we require Equations 1. Finally, the last necessary condition is that

$$\dot{\lambda}_H^j = (\rho + \delta)\,\lambda_H^j - \frac{\partial \mathcal{H}}{\partial H^j},$$

which gives us

$$\dot{\lambda}_S^j = (\rho+\delta)\,\lambda_S^j - \left(u^j\left(a_S^j, S\right) - \lambda_S^j \beta \sum_{k,h} \sigma_h^{j,k} C_h^{j,k}\left(\cdot\right) I_h^k + \sum_h \left(\lambda_{I_h}^j \left(\beta \tau_h^j \sum_{k,h} \sigma_h^{j,k} C_h^{j,k}\left(\cdot\right) I_h^k - \gamma_h^j I_h^j \right) \right) \right) \tag{9}$$

$$\dot{\lambda}_{I_A}^j = (\rho+\delta)\,\lambda_{I_A}^j - \left(u^j\left(a_{I_A}^j, I_A\right) - \sum_k \left(\lambda_A^k \beta \sigma_A^{k,j} C_A^{k,j}\left(\cdot\right) \right) + \sum_k \sum_h \left(\lambda_{I_h}^k \beta \tau_h^j \sigma_A^{k,j} C_A^{k,j}\left(\cdot\right) \right) \right) + \gamma_A^j \left(\kappa_A^j + \lambda_{I_A}^j \right) \tag{10}$$

$$\dot{\lambda}_{I_S}^j = (\rho+\delta)\,\lambda_{I_S}^j - \left(u^j\left(a_{I_S}^j, I_S\right) - \sum_k \left(\lambda_S^k \beta \sigma_S^{k,j} C_S^{k,j}\left(\cdot\right) \right) + \sum_k \sum_h \left(\lambda_{I_h}^k \beta \tau_h^j \sigma_S^{k,j} C_S^{k,j}\left(\cdot\right) \right) \right) + \gamma_S^j \left(\kappa_S^j + \lambda_{I_S}^j \right) \tag{11}$$

$$\dot{\lambda}_{I_H}^j = (\rho+\delta)\,\lambda_{I_H}^j - \left(u^j\left(a_{I_H}^j, I_H\right) - \sum_k \left(\lambda_H^k \beta \sigma_H^{k,j} C_H^{k,j}\left(\cdot\right) \right) + \sum_k \sum_h \left(\lambda_{I_h}^k \beta \tau_h^j \sigma_H^{k,j} C_H^{k,j}\left(\cdot\right) \right) \right) + \gamma_H^j \left(\kappa_H^j + \psi + \lambda_{I_H}^j \right) \tag{12}$$

whereby we need not partially differentiate the contact function with respect to the state variables due to our choice of matching technology. The solution to the planner's problem is then characterized by, for each j, Equations 1, Equations 6-8, Equations 9-12, and the boundary conditions

$$H^j\left(0\right) = H_0^j, \quad \lim_{t\to\infty} e^{-(\rho+\delta)t} \lambda_H^j H^j = 0. \tag{13}$$

To interpret Equation 6, note that the social planner balances two components. She balances the marginal increase in individual welfare from social activity by asymptomatic and susceptible individuals

$$S^j \frac{\partial u^j\left(a_S^{j*}, S\right)}{\partial a_S^j} + I_A^j \frac{\partial u^j\left(a_S^{j*}, I_A\right)}{\partial a_S^j}$$

with the marginal risk of a transferal from susceptibility to infected statuses across different subsets of the population

$$\lambda_S^j \beta S^j \sum_{k,h} \left(\sigma_h^{j,k} \frac{\partial C_h^{j,k}\left(a_S^{j*}, \cdot\right)}{\partial a_S^j} I_h^k \right) - \lambda_{I_A}^j \beta \tau_A^j S^j \sum_{k,h} \left(\sigma_h^{j,k} \frac{\partial C_h^{j,k}\left(a_S^{j*}, \cdot\right)}{\partial a_S^j} I_h^k \right)$$
$$+ \sum_{k \neq j} \left(\lambda_S^k \beta S^k \sigma_A^{k,j} \frac{\partial C_A^{k,j}\left(\cdot, a_S^{j*}\right)}{\partial a_S^j} I_A^j \right) - \sum_{k \neq j} \sum_h \left(\lambda_{I_h}^k \beta \tau_h^k S^k \sigma_A^{k,j} \frac{\partial C_A^{k,j}\left(\cdot, a_S^{j*}\right)}{\partial a_S^j} I_A^j \right).$$

As the social planner is unable to differentiate between susceptible and asymptomatic-infected individuals, she controls the contact level of these individuals in a way that factors in both the change in expected cost of infection due to a susceptible individual increasing their contact

$$\lambda_S^j \beta S^j \sum_{k,h} \left(\sigma_h^{j,k} \frac{\partial C_h^{j,k}\left(a_S^{j*}, \cdot\right)}{\partial a_S^j} I_h^k \right) - \lambda_{I_A}^j \beta \tau_A^j S^j \sum_{k,h} \left(\sigma_h^{j,k} \frac{\partial C_h^{j,k}\left(a_S^{j*}, \cdot\right)}{\partial a_S^j} I_h^k \right)$$

and the change in expected risk of infecting others due to an asymptomatic individual increasing their contact

$$\sum_{k \neq j} \left(\lambda_S^k \beta S^k \sigma_A^{k,j} \frac{\partial C_A^{k,j}\left(\cdot, a_S^{j*}\right)}{\partial a_S^j} I_A^j \right) - \sum_{k \neq j} \sum_h \left(\lambda_{I_h}^k \beta \tau_h^k S^k \sigma_A^{k,j} \frac{\partial C_A^{k,j}\left(\cdot, a_S^{j*}\right)}{\partial a_S^j} I_A^j \right).$$

In a similar vein, Equations 7-8 describes how the social planner balances individual welfare and the risk of infection for other infected individuals. Finally, to investigate the role that the social planner's information set plays in the optimal policy, I will also numerically evaluate the outcome for when the social planner can only control $a_S^j = a_{I_A}^j = a_{I_S}^j, a_{I_H}^j$ and $a_S^j = a_I^j$.

2.3 Laissez-Faire Equilibrium

In the laissez-faire equilibrium, individuals take the social activity and health states of others as given, denoted by A_h^j and H^j. They have rational beliefs about their own probabilities of being in each infection state, which I denote by h^j, where h is the infection state. I assume

that they cannot differentiate when they are susceptible and infectious yet asymptomatic. Individuals then solve

$$\max_{\left\{a_S^j, a_{I_S}^j, a_{I_H}^j, a_R^j\right\}_{j\in\mathcal{J}}} \int_0^\infty e^{-(\rho+\delta)t} \sum_j \Big[s^j u^j\left(a_S^j, s\right) + i_A^j u^j\left(a_S^j, i_A\right) + i_S^j u^j\left(a_{I_S}^j, i_S\right) + i_H^j u^j\left(a_{I_H}^j, i_H\right) + r^j u^j\left(a_r^j, r\right) - \sum_h \left(\gamma_h^j i_h^j \left(\kappa_h^j + \psi_h\right)\right) \Big] \, dt \tag{14}$$

subject to the epidemiological dynamics

$$\begin{aligned}
\dot{s^j} &= -\beta s^j \sum_{k,h} \sigma_h^{j,k} C_h^{j,k}\left(a_s^j, A_{I_h}^k\right) I_h^k, \\
\dot{i_h^j} &= \beta \tau_h^j s^j \sum_{k,h} \sigma_h^{j,k} C_h^{j,k}\left(a_s^j, A_{I_h}^k\right) I_h^k - \gamma_h^j i_h^j, \\
\dot{r^j} &= \sum_h \left(1 - \pi_h^j\right) \gamma_h^j i_h^j, \\
\dot{d^j} &= \sum_h \pi_h^j \gamma_h^j i_h^j,
\end{aligned} \tag{15}$$

The laissez-faire equilibrium is then characterized when the individual choice of social activity and the aggregate choice of social activity are equal. The optimality conditions for the problem facing the individual are similar to that of the social planner's problem, with a few differences. First, a change in social activity of an individual has a smaller impact on the change in the shadow cost of susceptibility and infection. For example, for each j, we have

$$\begin{aligned}
&s^j \frac{\partial u^j\left(a_S^{j*}, s\right)}{\partial a_S^j} + i_A^j \frac{\partial u^j\left(a_S^{j*}, i_A\right)}{\partial a_S^j} - \lambda_s^j \beta s^j \sum_{k,h} \left(\sigma_h^{j,k} \frac{\partial C_h^{j,k}\left(a_S^{j*}, \cdot\right)}{\partial a_S^j} I_h^k \right) \\
&+ \lambda_{i_A}^j \beta \tau_A^j s^j \sum_{k,h} \left(\sigma_h^{j,k} \frac{\partial C_h^{j,k}\left(a_S^{j*}, \cdot\right)}{\partial a_S^j} I_h^k \right) = 0
\end{aligned} \tag{16}$$

instead of Equation 6. This means that the individual does not consider the change in cost of transitioning from susceptibility to infection for other individuals due to a change in their behavior, whereas the social planner does. Second, the individual does not internalize the

social cost of infection spread. For example, for each j, the costate equation for symptomatic infection for an individual is

$$\dot{\lambda}^j_{i_S} = (\rho + \delta)\,\lambda^j_{i_S} - u^j\left(a^j_{i_S}, i_S\right) + \gamma^j_S\left(\kappa^j_S + \lambda^j_{i_S}\right) \tag{17}$$

instead of Equation 11. The social planner, contrary to the individual, understands that the shadow cost of each disease state is influenced by the change in infection spread within the population.

2.4 Testing

In reality, the social planner's information and identification of infected individuals may be highly imperfect. This creates a role for testing and contact tracing. To explore the role of testing in an optimal policy, I start by examining the extremes: in a universe with no testing and a public that perfectly follows the social planner's policy, the social planner solves the problem as outlined in Section 2.2 with $a_{I_S} = a_{I_A} = a_S$. In a regime that freely and perfectly tests and traces all individuals, the social planner has perfect information on the health status of all individuals and therefore solves the problem

$$\begin{aligned}\max_{\left\{a^j_S, a^j_{I_A}, a^j_{I_S}, a^j_{I_H}, a^j_R\right\}_{j\in\mathcal{J}}} \int_0^\infty e^{-(\rho+\delta)t} \sum_j \Big[& S^j u^j\left(a^j_S, S\right) + I^j_A u^j\left(a^j_{I_A}, I_A\right) + I^j_S u^j\left(a^j_{I_S}, I_S\right) \\ & + I^j_H u^j\left(a^j_{I_H}, I_H\right) + R^j u^j\left(a^j_R, R\right) \\ & - \sum_h \left(\gamma^j_h I^j_h\left(\kappa^j_h + \psi_h\right)\right) \Big]\, dt\end{aligned} \tag{18}$$

subject to the dynamic constraints in Equations 1. The necessary conditions for optimality no longer follow Equation 6. Instead, they are separated into

$$S^j \frac{\partial u^j\left(a^{j*}_S, S\right)}{\partial a^j_S} - \lambda^j_S \beta S^j \sum_{k,h}\left(\sigma^{j,k}_h \frac{\partial C^{j,k}_h\left(a^{j*}_S, \cdot\right)}{\partial a^j_S} I^k_h\right) = 0 \tag{19}$$

and

$$I_A^j \frac{\partial u^j\left(a_{I_A}^{j*}, I_A\right)}{\partial a_{I_A}^j} + \lambda_{I_A}^j \beta \tau_A^j S^j \sum_{k,h}\left(\sigma_h^{j,k} \frac{\partial C_h^{j,k}\left(a_{I_A}^{j*}, \cdot\right)}{\partial a_{I_A}^j} I_h^k\right) - \sum_{k \neq j}\left(\lambda_S^k \beta S^k \sigma_A^{k,j} \frac{\partial C_A^{k,j}\left(\cdot, a_{I_A}^{j*}\right)}{\partial a_{I_A}^j} I_A^j\right)$$
$$+ \sum_{k \neq j} \sum_h \left(\lambda_{I_h}^k \beta \tau_h^k S^k \sigma_A^{k,j} \frac{\partial C_A^{k,j}\left(\cdot, a_{I_A}^{j*}\right)}{\partial a_{I_A}^j} I_A^j\right) = 0 \tag{20}$$

This reflects that in a regime with free and perfect testing, the social planner's information set changes and therefore no longer has to jointly consider the impacts of controlling contact levels of susceptible and asymptomatic individuals. In reality, testing is costly and partial. Testing and contact tracing serve two purposes for public health: to identify infected individuals and to inform public health officials of the trajectory of the pandemic within an area. Contact tracing similarly identifies infected individuals based on contacts of individuals already identified as infected. However, these methods are necessarily incomplete as contact tracing and testing the entire population is extremely costly.

I now turn to model a targeted random testing program where the social planner tests the non-recovered and non-hospitalized population of different age groups at random. This is most similar to surveillance testing programs where some proportion of the population are tested at a regular schedule. Let χ be the (linear) constant cost of identifying one non-hospitalized individual[8], and let ζ^j be the percent of non-hospitalized individuals in group j tested per period t. Then in each instantaneous period and for each j, $\zeta^j\left(\left(I_A^j + I_S^j\right) / \left(I_A^j + I_S^j + S^j\right)\right)$ individuals are identified, so that ζ^j proportion of asymptomatic and symptomatic individuals follow the optimal level of social activity $a_{I_A}^*, a_{I_S}^*$[9].

[8]In reality, the costs of testing and contact tracing are unlikely to be linear or constant. For example, there are large fixed costs to implement a testing and contact tracing regime: Developing the requisite test and sequencing the genome of the virus, setting up facilities for drive-by testing, and getting funding for testing and contact tracing programs all represent high initial fixed costs. As such it is possible that the high initial fixed costs render testing and contact tracing programs non-optimal even if future variable costs are low. Here I use the linear, constant assumption for simplicity, especially as there is currently a lack of data and quantitative assessment of the costs and efficacy of US testing and contact tracing programs. However, better data may allow us to model the costs of testing and contact tracing more effectively in the future to better understand the effects of a high initial fixed cost on optimal policy.

[9]There is a small amount of literature that models contact tracing during COVID-19 with agent-based modeling. See for example Almagor and Picascia, (2020). However it is difficult to incorporate their approach

Due to random matching, we may simply enforce the constraint on the social planner that

$$a_{I_A}^j = \left(1-\zeta^j\right) a_S^j + \zeta^j a_{I_A}^{j*} \tag{21}$$

where $a_{I_A}^{j*}$ denotes the target level of social activity by the social planner. For simplicity and to limit the dimension of the control space, I set $a_{I_A}^{j*} = a_{I_S}^{j*}$. Hence the social planner facing a decision over testing solves the problem

$$\begin{aligned}\max_{\left\{a_S^j, a_{I_A}^{j*}=a_{I_S}^{j*}, a_{I_H}^j, \zeta^j\right\}_{j\in\mathcal{J}}} \int_0^\infty e^{-(\rho+\delta)t} \Bigg[\sum_j \Big[\left(S^j + \left(1-\zeta^j\right)\left(I_A^j + I_S^j\right)\right) u^j\left(a_S^j, S\right) + \zeta^j I_A^j u^j\left(a_{I_A}^{j*}\right) \\ + \zeta^j I_S^j u^j\left(a_{I_S}^{j*}\right) + I_H^j u^j\left(a_{I_H}^j, I_H\right) \\ - \sum_h \left(\gamma_h^j I_h^j \left(\kappa_h^j + \psi_h\right)\right) \Big] - \chi \sum_j \zeta^j \left(I_A^j + I_S^j + S^j\right) \Bigg] \, dt\end{aligned} \tag{22}$$

subject to the dynamic constraints in Equations 1, except with activity from non-hospitalized individuals replaced with Equation 21. Observe that if $\zeta = 0$ then we revert to the problem facing the social planner with no testing. If $\sum \zeta = 1$ and $\chi = 0$ then we revert to the problem as outlined in Equation 18. To gain insight into this problem, we derive one of the necessary conditions

$$\begin{aligned}\left(I_A^j + I_S^j\right) u^j\left(a_{I_A}^{j*}\right) - \left(I_A^j + I_S^j\right) u^j\left(a_S^j, S\right) = \chi\left(I_A^j + I_S^j + S^j\right) \\ + \left(\lambda_S^j \beta S^j \sum_k \left(\sigma_A^{j,k} \frac{\partial C_A^{j,k}(\cdot)}{\partial \zeta^j} I_A^k\right)\right) \\ - \left(\lambda_{I_A}^j \left(\beta \tau_A^j S^j \sum_k \sigma_A^{j,k} \frac{\partial C_A^{j,k}(\cdot)}{\partial \zeta^j} I_A^k - \gamma_A^j I_A^j\right)\right)\end{aligned} \tag{23}$$

This equation describes that the optimal policy will weigh the cost of testing with the

in my model and I opted to simplify the mechanism in which the social planner identifies asymptomatic individuals and quarantine them, focusing only on testing.

decrease in personal welfare of asymptomatic individuals due to increasing testing and the expected reduction in risks from limiting the contacts of asymptomatic individuals.

2.5 Imperfect Enforcement

In reality, the social planner may not be able to perfectly enforce her optimal policy, as people may disobey social distancing or lockdown guidelines, escape quarantine, or socially gather in secret. Furthermore, an optimal policy that attempts to enforce some $\bar{a}$ social activity level on individuals may be infeasible if $\bar{a}$ implies the disability of getting groceries or even going to the hospital when getting sick (as a hospital is a place with highly dense social activity). Modeling imperfect enforcement by using a convex combination of the social planner's target social activity and the individual's laissez-faire optimal level of social activity will only compel the social planner to impose much lower targets for social activity, as she takes into account her own imperfect enforcement[10]. Therefore, I assume that the social planner has already taken into account this form of imperfect enforcement so that the level of social activity in each individual type is the same as that of her actual target level. Hence, I model the other facet of imperfect enforcement by constraining the social planner's controls. She then solves Equation 22 subject to the altered dynamic constraints in Equations 1 modified by Equation 10 and the additional control variable constraints:

$$\begin{aligned} a_S^j &\geq \bar{a} \\ a_{I_S}^j &\geq \bar{a} \\ a_{I_H}^j &\geq \bar{a} \end{aligned} \tag{24}$$

We then have three more costate variables $\mu_S, \mu_{I_S}, \mu_{I_H}$ and they will appear on the right-hand-side of the equivalent formulations for the necessary optimal conditions Equations 6-8

[10]It is possible that real-world governments have failed to factor in this type of imperfect enforcement in their policies. Moreover, enforcement capability can decay over time. COVID fatigue has heightened for many people and optimal policy may need to take into account changes in adherence over time. See for example Crane et al., (2021) for evidence of adherence decay. However, I will not investigate this phenomenon in this paper.

for this problem, replacing 0 with $\mu_H\left(a_H^j - \bar{a}\right)$.

3 Numerical Illustration

3.1 Calibration

I detail the computational method in Section A. I start by examining the basic model in Section 2.2. First, let there be 3 different individual types: y, m, and o denoting young, middle-aged, and old respectively, so that $\mathcal{J} = \{y, m, o\}$. Specifically, I let young be defined as 1-29 years of age, middle-aged be defined as 30-65 years of age, and old be defined as 65+ years of age. Note that due to the heterogeneity in how different articles and data sources divide data by age, in general my calibration can only be treated as approximate. As discussed, I use a quadratic contact function, i.e. $C_h^{j,k}\left(a_S^j, a_h^k\right) = a_S^j a_h^k$. I set the utility representation to $u^j\left(a_H, H\right) = \log a_H - a_H + h_H^j$. For the basic model, I calibrate as follows in Tables 1 and 2.

Parameter Description	**Parameter**	**Calibration**
Optimal level of contact for susceptible, asymptomatic, and symptomatic individuals	$h_S = h_{I_A} = h_{I_S}$	1
Optimal contact for hospitalized individuals	h_{I_H}	0.8
Base infection doubling rate	β	1/2.68
Recovery rate for asymptomatic individuals	γ_A	1/6
Recovery rate for symptomatic individuals	γ_S	1/10
Recovery rate for hospitalized individuals	γ_H	1/23
Homophilic parameter	σ	1
Discount rate	ρ	0.05/365
Arrival rate of cure	δ	0.67/365
Asymptomatic rate in young individuals	τ_A^y	0.79
Symptomatic rate in young individuals	τ_S^y	0.206398
Hospitalization rate in young individuals	τ_H^y	0.003602
Asymptomatic rate in middle-aged individuals	τ_A^m	0.5
Symptomatic rate in middle-aged individuals	τ_S^m	0.43545
Hospitalization rate in middle-aged individuals	τ_H^m	0.06455
Asymptomatic rate in old individuals	τ_A^o	0.31
Symptomatic rate in old individuals	τ_S^o	0.526
Hospitalization rate in old individuals	τ_H^o	0.164

Table 1
Parameter calibration for the basic model.

Parameter Description	**Parameter**	**Calibration**
Infection fatality rate for young, asymptomatic	π_A^y	0
Infection fatality rate for young, symptomatic	π_S^y	4.102×10^{-4}
Infection fatality rate for young, hospitalized	π_H^y	0.013
Infection fatality rate for middle-aged, asymptomatic	π_A^m	0
Infection fatality rate for middle-aged, symptomatic	π_S^m	5.049×10^{-4}
Infection fatality rate for middle-aged, hospitalized	π_H^m	0.060
Infection fatality rate for old, asymptomatic	π_A^o	0
Infection fatality rate for old, symptomatic	π_S^o	0.0376
Infection fatality rate for old, hospitalized	π_H^o	0.188
Value of a statistical life	v	31755
Cost of hospitalization	ψ/γ_H	116.8
Minimal enforcement	$\bar{a}$	0.1554
Parameter Description	**Derived Parameter**	**Derived Calibration**
Expected cost of death conditional on infection	κ	$\kappa_h^j = \pi_h^j \cdot v$
Daily cost of hospitalization	ψ	5.078

Table 2
Parameter calibration for the basic model.

3.1.1 Optimal level of contact

The optimal level of contact is normalized to 1 for a healthy individual. I assume that asymptomatic individuals, given that they do not experience symptoms, wish to engage in the same level of social activity whether or not they know they are infected. It is less reasonable to assume that symptomatic individuals wish to engage in the same level of vigor as healthy individuals. However, I assume as such to control the dimension of the control space as mentioned in Section 2.4. In general, because such symptomatic individuals are not hospitalized and therefore have milder symptoms, it is reasonable to expect that they would also prefer to engage close to the level of social activity as that of asymptomatic individuals, making an equality approximately true. Finally, the optimal level of contact for hospitalized individuals is set at 0.8.

3.1.2 Base infection doubling rate

I calibrate β to $1/2.68$, following Lurie et al.'s estimation of the mean epidemic doubling time before widespread mitigation efforts (the figure is calibrated to their corrected data).

3.1.3 Recovery rates

I calibrate γ according to Cevik et al., a meta study on viral load dynamics. Specifically, I used the shedding duration rather than ICU times for the calibration as γ is used to calibrate the disease dynamics in the model rather than to capture health outcomes of individuals. I then took the average of the shedding duration by severity across the studies that examined the relationship between severity of illness and viral dynamics. Then, $\gamma = 1/t$, where t is the days of viral shedding. As far as the author is aware, there is no data on the shedding duration of COVID-19 by the combination of age and illness severity[11].

[11]Except when patients are hospitalized. See CDC data(CDC, 2020) for figures on differences in illness duration by age conditional on hospitalization. The data suggests that conditional on illness severity, there is not much difference in recovery time. Rather, different age groups are heterogeneous in illness severity itself.

3.1.4 Homophilic parameter

I calibrate σ to 1 for no homophilia. In Section 3.7 I will investigate whether homophilic preferences may impact optimal policy and the trajectory of the pandemic.

3.1.5 Discount rates

I calibrate ρ to 0.05/365 and δ to 0.67/365 following Farboodi et al.. Note that the calibration of δ is in line with the reality in 2021. Indeed, Phase 2 of Chicago's vaccine program will take place from April 19, 2021 to June 2021 (*Vaccine Distribution Phases*, n.d.) which is close to the expectation of 1.5 years at the start of the pandemic.

3.1.6 Asymptomatic, symptomatic, hospitalization and infection fatality rates

Given the scarcity of data on the real rates of these figures I calibrated several of these parameters by inference. First, I follow Davies et al. and calibrate asymptomatic rates based on their estimation of COVID-19 symptomatic rates across different age groups. The weighted average of asymptomatic rate is then 0.580. This calibration is roughly in line with that of other studies that do not estimate by age groups, including Yang et al. (0.423), and also fits the trend that asymptomatic patients tend to be younger (Yang et al., (2020)). However, due to the lack of data on the infection fatality rates by the combination of infection severity and age, I make a critical assumption that the fatality rates for asymptomatic rates are sufficiently low that calibrating $\pi_A = 0$ will not influence the numerical results of the model disproportionately[12]. With this assumption, we can then deduce the symptomatic rate and infection fatality rate for symptomatic, but not hospitalized individuals. I follow Verity et al. for the overall infection fatality rate and hospitalization rate, based on the aggregate time series of cases in mainland China, adjusted for censoring, demography, and under-ascertainment. This gives us $\pi^y = 1.315 \times 10^{-4}$, $\pi^m = 0.008415$, and $\pi^o = 0.0506$. The

[12]This is false in reality. For example, COVID-19 induced hypercoagulability in an individual with asymptomatic history, leading to their death (Del Nonno et al., (2021)). However the data largely suggests that the death rate of asymptomatic individuals is minimal (Gao et al., (2021)).

similarly adjusted hospitalization rates are $\tau_H^y = 0.003602$, $\tau_H^m = 0.06455$, and $\tau_H^o = 0.164$. To find the rest of the parameters, we require an estimate for π_H^j, i.e. the hospitalization fatality rate. I use the CDC planning scenario estimated dataset (CDC, 2020) to derive $\pi_H^y = 0.013$, $\pi_H^m = 0.060$ and $\pi_H^o = 0.188$. We can then back out τ_S^j with $\tau_S^j = 1 - \tau_H^j - \tau_A^j$ and $\pi_A^j \cdot \tau_A^j + \pi_S^j \cdot \tau_S^j + \pi_H^j \cdot \tau_H^j = \pi^j \implies \pi_S^j = \left(\pi^j - \pi_H^j \cdot \tau_H^j\right) / \tau_S^j$.

3.1.7 Cost of hospitalization

I follow Bartsch et al. in my calibration for the cost of hospitalization for each hospitalized individual. They find no substantial heterogeneity in direct hospitalization costs ($11367-$15943) and so I use the weighted average $14366 for the calibration. This converts into 116.8 in the model's units. Note that the disadvantage in this calibration is that there is no accurate data that factors in indirect costs from hospitalizations and infections. Indeed, the meta-study by Lopez-Leon et al. reveals that a significant proportion of symptomatic or hospitalized individuals suffer from so-called "long-hauler" syndromes, such as fatigue (58%) and attention disorder (27%), both of which are symptoms that may impact labor productivity and require further medical treatment and thus costs. However, given the lack of data on the exact costs incurred by these "long-hauler" syndromes, I will not attempt to factor them into the calibration. Further research on "long-hauler" syndromes and their economic costs may be appropriate in the future when there is more data.

3.1.8 Minimal enforcement

For simplicity, I set the minimal enforcement the social planner may achieve at 0.1554. Supposing all individuals have a social activity of 0.1554 for all t, the social planner's objective function then evaluates to -443.4, equal to the evaluated objective function in an economy with no behavioral response to the pandemic. In this sense, the social planner is not allowed to set any individual's level of social activity below the point at which society is better off not reacting to the virus if every individual is subject to the same level of social activity. In

Section 3.8 I examine how other values of $\bar{a}$ may impact the social planner's optimal policy.

3.1.9 Initial conditions

I calibrate for the initial conditions on March 21, 2020, shown in Table 3. First I use the U.S. Census Data's estimates on April 1, 2020 (Bureau, n.d.) to derive that 54,303 thousands people are old (65+ years old), 150,452 thousands people are middle-aged (30-64 years old), and 127,844 thousands people are young (1-29 years old). This gives us $Y(0) = S^y(0) + I^y(0) + R^y(0) = 127844/(127844 + 150452 + 54303) = 0.3844$, $M(0) = 0.4524$, and $O(0) = 0.1632$. I then infer the share of susceptible, asymptomatic, symptomatic, hospitalized, and recovered individuals as follows: I start by subsetting CDC data on deaths (Calgary, n.d.) on an end date of March 21, 2020. Given that most people who die are hospitalized and that the shedding duration of hospitalized individuals average at 23 days, the infections inducing the deaths at March 21, 2020 are very likely to be unaffected by the start of social distancing guidelines on March 13, 2020. Given the overall infection fatality rate and asymptomatic, symptomatic, and hospitalization rates we can then back out the initial conditions on March 21, 2020. In particular, based on the median illness duration of 10 days (Wortham, 2020) from February to May 2020, we can then derive $R_0 = \beta/\gamma = (10/2.68) = 3.73$ for our calibration.

For example, the CDC data records 5 (5/332599000) deaths from individuals aged 0 to 29. Given an overall infection fatality rate within this group of 1.315×10^{-4}, we can estimate that 38018 (38018/332599000) young individuals are recovered on March 21, 2020. Following the dynamics of the SIR model, we can back out that

$$1 - R(0) - D(0) - \exp\left(-R_0\left(R(0) + D(0)\right)\right) = 0.000311995$$

which we can then multiply by the respective rates for each sub-state of infection. Finally, using $Y - I(0) - R(0) - D(0)$ gives us $S(0)$, where Y is the number of young people within

Parameter Description	Parameter	Calibration
Initial susceptible young individuals	$S^y(0)$	0.3839737
Initial asymptomatic young individuals	$I_A^y(0)$	0.0002465
Initial symptomatic young individuals	$I_S^y(0)$	6.440×10^{-5}
Initial hospitalized young individuals	$I_H^y(0)$	1.124×10^{-6}
Initial recovered young individuals	$R^y(0)$	0.0001143
Initial dead young individuals	$D^y(0)$	1.503×10^{-8}
Initial susceptible mid-aged individuals	$S^m(0)$	0.45222
Initial asymptomatic mid-aged individuals	$I_A^m(0)$	6.388×10^{-5}
Initial symptomatic mid-aged individuals	$I_S^m(0)$	5.563×10^{-5}
Initial hospitalized mid-aged individuals	$I_H^m(0)$	8.247×10^{-6}
Initial recovered mid-aged individuals	$R^m(0)$	4.641×10^{-5}
Initial dead mid-aged individuals	$D^m(0)$	3.939×10^{-7}
Initial susceptible old individuals	$S^o(0)$	0.163102
Initial asymptomatic old individuals	$I_A^o(0)$	2.212×10^{-5}
Initial symptomatic old individuals	$I_S^o(0)$	3.754×10^{-5}
Initial hospitalized old individuals	$I_H^o(0)$	1.170×10^{-5}
Initial recovered old individuals	$R^o(0)$	2.482×10^{-5}
Initial dead old individuals	$D^o(0)$	1.323×10^{-6}

Table 3
Calibration for initial conditions for the basic model.

the population.

3.1.10 VSL

I calibrate the VSL following Farboodi et al. and Hall et al.[13]. In particular, this implies that a unit of utility in my model has an equivalent US dollar rate of around 123. Note that I implicitly assume that hospitalized individuals do not permanently wish to have social activity at a level of a_H^*, so that

$$\frac{\log(1)}{\hat{\rho}} - 0.001v \neq \frac{\log(a_H^* - 31.755\hat{\rho})}{\rho}$$

[13]I follow Farboodi et al.'s strategy in calibration, detailed in Section 5.1 of their paper. Note that the "exchange rate" from model utils to US dollars is identical due to usage of the same utility form.

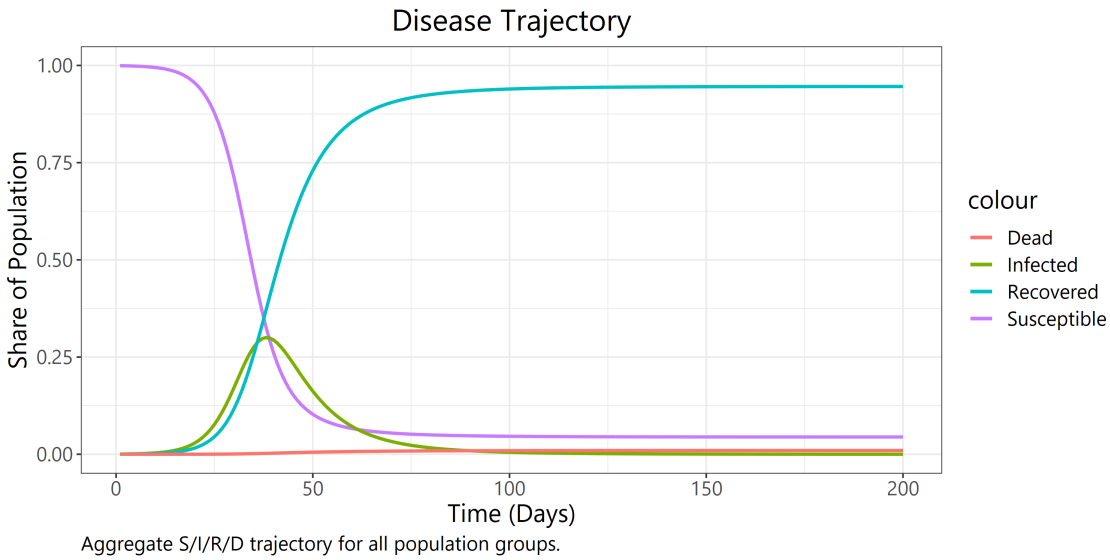

Figure 2
Disease Trajectory with no behavioral responses

3.2 Basic Heterogeneous SIRD model

As in the homogeneous SIRD model with no behavioral responses, the disease trajectory (Figure 2) implies achieving mass herd immunity by a little more than 50 days. Indeed, the pandemic is virtually over by the 100th day, with over 95% of the population either dead or recovered from the virus. With no behavioral responses, the cumulative deaths are also extremely high (Figure 3), with 4.9% among the old population, 0.39% among the middle-aged population, and 0.014% among the young population, for a weighted total of 0.97% of the population dead by the end of the pandemic. This benchmark result illustrates the worst-case scenario of letting the virus go unchecked and is also unlikely an accurate depiction of reality.

3.3 Laissez-Faire Equilibrium

Under the laissez-faire equilibrium, individuals in each age group exhibit vastly different behavior. At the beginning of the pandemic, as the young population has a lower expected cost of infection than that of the old population, they have a higher level of social activity. As opposed to the social optimum, the high levels of social activity causes infection rates to rise.

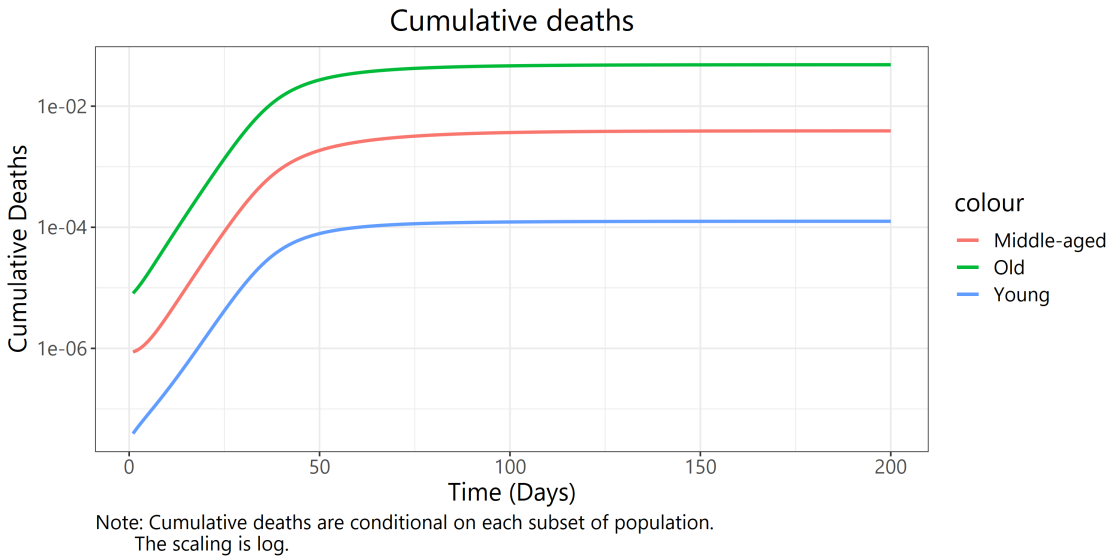

Figure 3
Cumulative deaths with no behavioral responses

In response, an old individual decreases social activity as infections peak, hitting the minimal level possible. Note that with our calibrations, older individuals are disproportionately affected by the negative externality posed by the young population who are maintaining nearly the same level of social activity as they would outside a pandemic.

3.4 Social Optimum

Optimal policy under a social planner entails significant curtail of social activity (Figure 8), regardless of the set of controls the social planner is afforded. In all three scenarios, social activity is curtailed for a much longer time than that of the basic SIRD model in order to flatten the curve. Intuitively, this is due to the high discounting rate of the objective function. Optimal policy compels the social planner to flatten the curve and curb social activity at a rate that would not otherwise be sustained were ρ the only discounting factor, because individuals in the economy expect at a daily rate of δ to be cured and enter the universe in which everyone is immediately immune and recovered. In other words, individuals in this economy are expecting with high probability to not actually have to experience prolonged periods of low levels of social activity as dictated by the social planner. This leads to a much

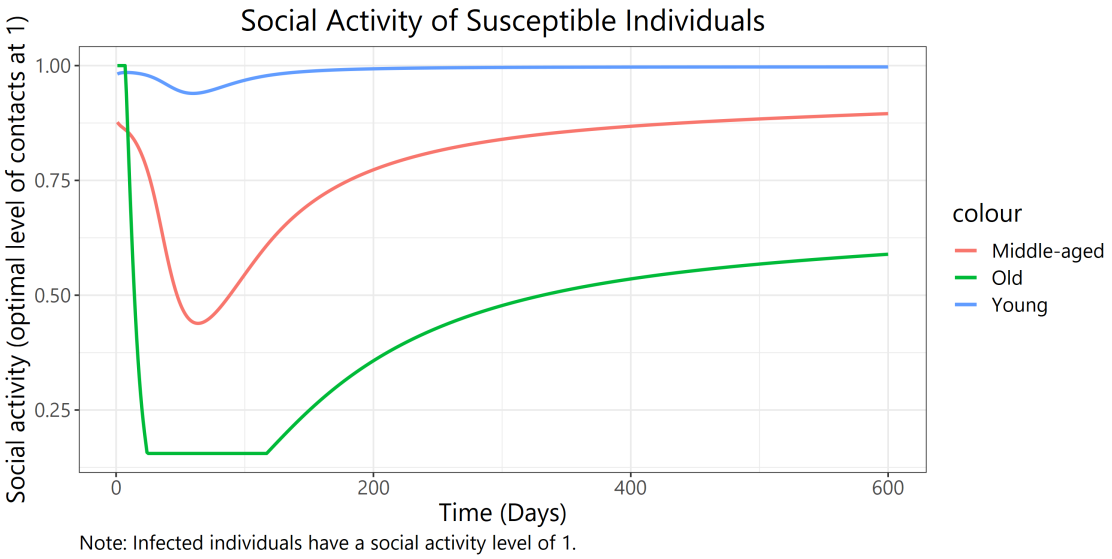

Figure 4
Social activity under laissez-faire

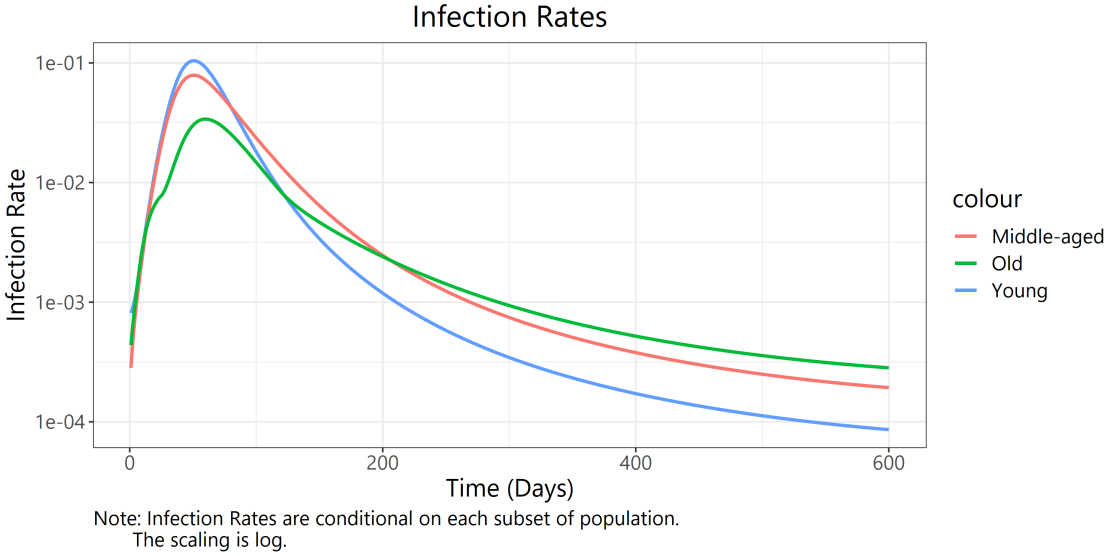

Figure 5
Infections under laissez-faire

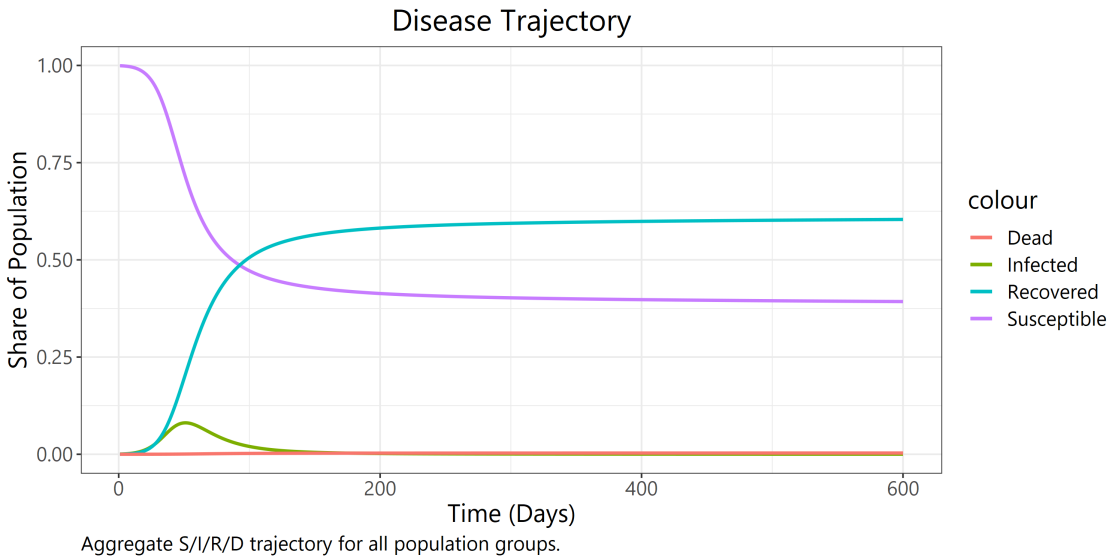

Figure 6
Disease Trajectory under laissez-faire

lower infection rate that persists for a prolonged period (Figures 9). The heterogeneity in infection rates across different age groups is due to the heterogeneity in infection sub-states. In particular, because older individuals are more likely to be hospitalized or symptomatic, which have a longer viral shedding duration than that of an asymptomatic individual, for each infection acquired by an older individual, the infection will last longer and therefore increase the daily infection rate. Naturally, the overall low infection rates also lead to lower deaths and similarly a prolonged period of high susceptibility (Figures 10).

Yet, despite the flattened infection rates, the reproduction number never escapes far from 1.0 (Figures 11). As the social planner internalizes the externality that each individual in the economy poses, she sets levels of social activity in such a way as to balance the externality (the risk due to increasing infection rate) just so as to buy time for the cure. In this sense, we can explain why the $R(t)$ number never strays far from 1. First, it does not go above 1 because the increase in infections impose a negative externality that is costly enough that it is better off traded with imposing less costly lockdowns. It also does not go below 1 because the social planner recognizes that the value from curbing the virus altogether (by going much below 1) is insufficiently high due to the imminence of a vaccine that can curb

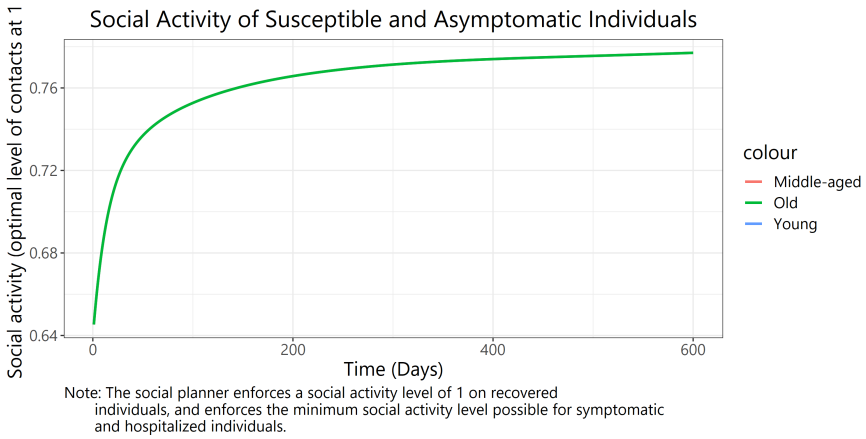

Figure 7
Social activity level for a social planner that controls susceptible, symptomatic, and hospitalized social activity, without heterogeneity in age

the virus anyways. Together, these factors explain why the social planner will optimize in such a way as to never crush the virus nor allow it to get out of control.

The difference in welfare and costs for targeted and untargeted (by age) policies in this model is small, ranging from 2% to 6% (see Tables 4 and 5). In contrast to the laissez-faire equilibrium, social optimum allows all age groups to have a social activity level that is relatively close to each other. In the homogeneous case, the social planner chooses a social activity path that is near the middle of the social activity paths chosen in the heterogeneous case. In effect, the decrease in utility from social activity for young people from switching from a targeted policy to an untargeted policy is balanced by the increase in utility from social activity for old people. Similarly, the increase in risk from increasing social activity for old people is balanced by the decrease in risk from decreasing social activity for young people from switching to the untargeted policy. This explains how the welfare gain from targeted policies by age is small. However, in the model units, the savings generated from a targeted policy can be significant when put in context of the entire US. In the case where the social planner has information on the infection state of hospitalized individuals only, the aggregate savings from instituting a targeted policy is $220 per capita, which is equivalent to an aggregate savings of $72 billion.

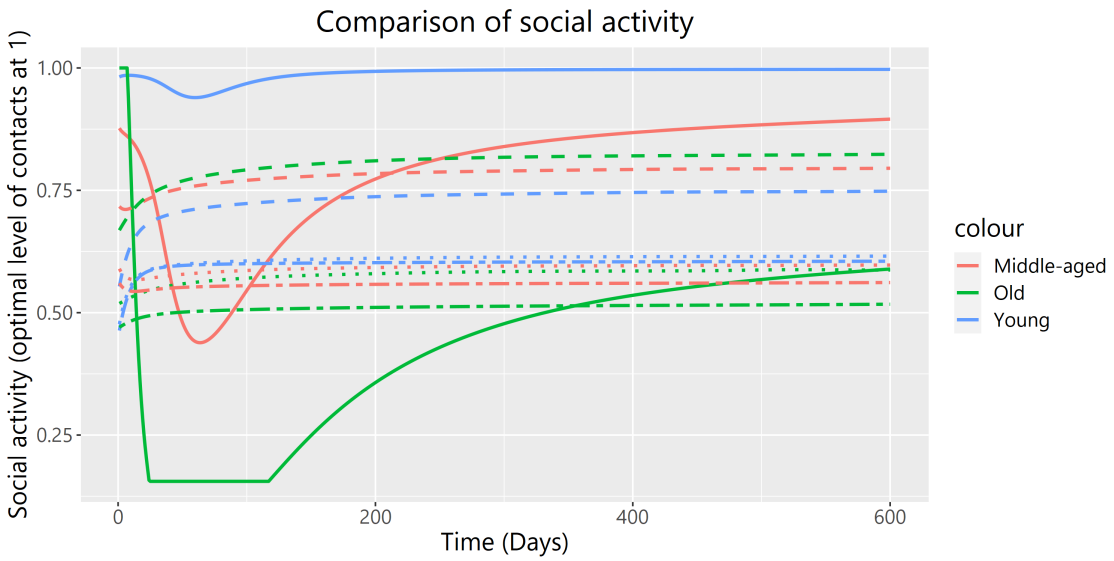

Figure 8

Social activity level for susceptible and non-identified infected individuals. The solid line corresponds to the laissez-faire equilibrium. The dashed line corresponds to the social activity for the information set $a_S = a_{I_A}, a_{I_S}, a_{I_H}$. The dotted line corresponds to the social activity for the information set $a_S = a_{I_A} = a_{I_S}, a_{I_H}$. The dot-dash line corresponds to the information set $a_S = a_{I_A} = a_{I_S} = a_{I_H}$. Identified infected individuals have a social activity level of 1 under laissez-faire, and a social activity level of $\bar{a}$, the minimal enforcement, under social optimum.

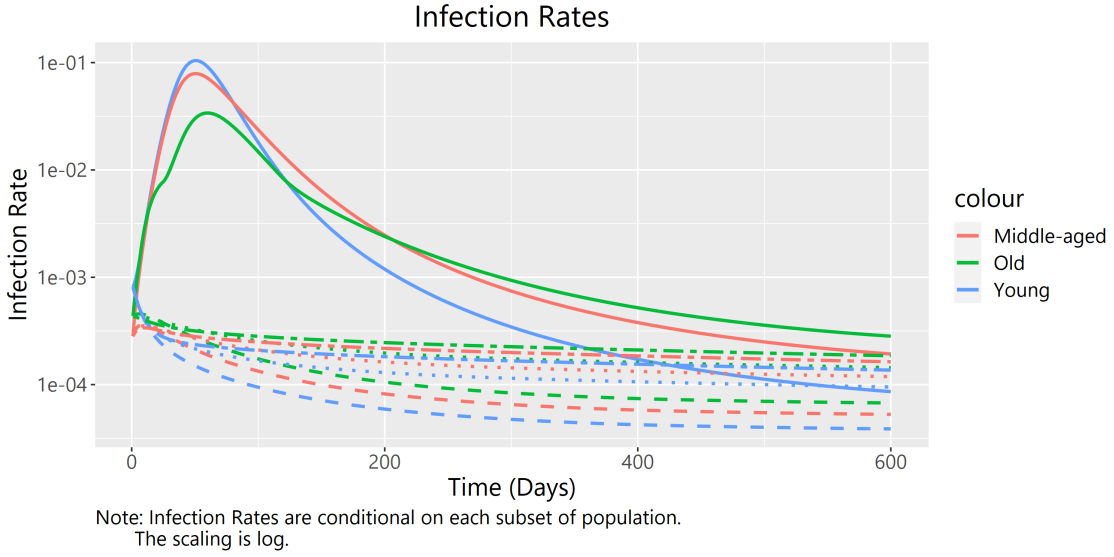

Figure 9

Infection rates. The line types correspond to the same scenarios as in Figure 8.

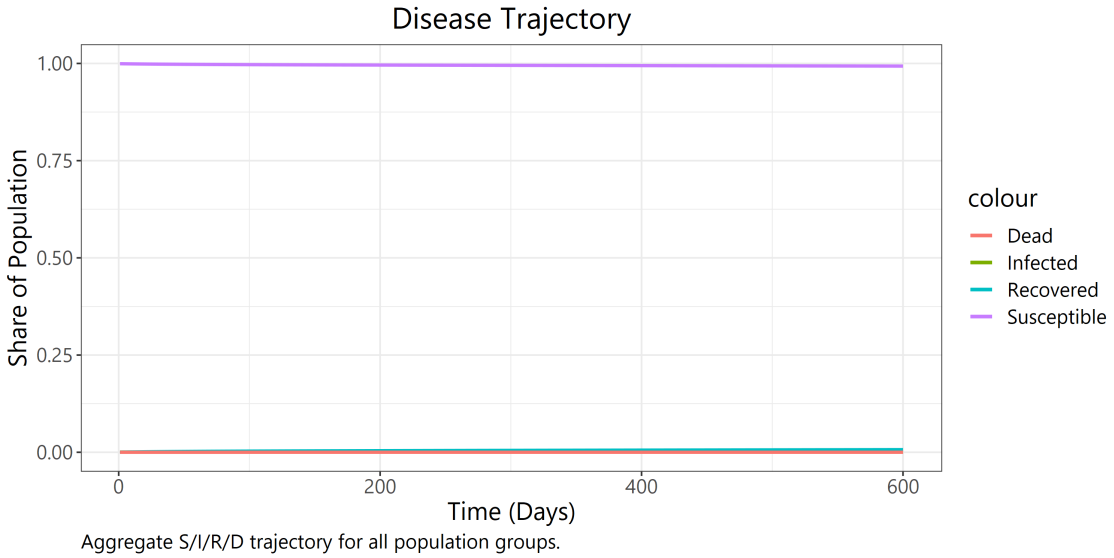

Figure 10
Disease dynamics for a social planner that controls susceptible, symptomatic, and hospitalized social activity

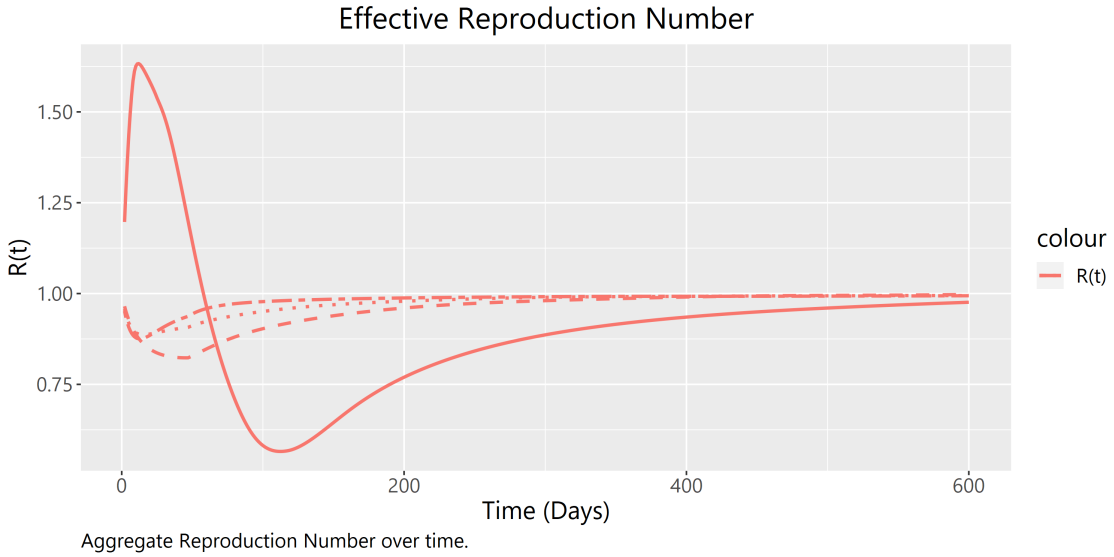

Figure 11
$R(t)$. The line types correspond to the same scenarios as in Figure 8.

Information Set	**Welfare**	**Cumulative Deaths at Day 600**
$a_S = a_{I_A}, a_{I_S}, a_{I_H}$	-16.192	7.536×10^{-5}
$a_S = a_{I_A} = a_{I_S}, a_{I_H}$	-51.577	0.000129
$a_S = a_{I_A} = a_{I_S} = a_{I_H}$	-61.568	0.000158
$a_S = a_{I_A}, a_{I_S}, a_{I_H}$, homogeneous	-16.991	7.655×10^{-5}
$a_S = a_{I_A} = a_{I_S}, a_{I_H}$, homogeneous	-53.347	0.000131
$a_S = a_{I_A} = a_{I_S} = a_{I_H}$, homogeneous	-65.702	0.000161
Laissez-faire	-113.241	0.00320
Basic SIRD model	-308.816	0.00971

Table 4
Welfare and cumulative deaths for different information sets

3.5 Information Sets

The information that a social planner has also informs the optimal policy that she should pursue. In particular, it should not be surprising that welfare is maximized for the social planner that can control the most variables, since that social planner can always never do worse than a social planner that can control fewer variables, given that she can always at least choose the optimizer for the social planner with less controls (Table 4). Note that deaths are nearly halved for and welfare is significantly increased for a social planner that is able to identify susceptible and hospitalized individuals and impose lockdown specifically on those individuals. In reality, it is more likely that a social planner faces constraints close to that of the information set wherein the social planner can only impose lockdown on hospitalized individuals and non-hospitalized individuals. Furthermore, note that it is optimal for the social planner to impose the minimum enforcement level on identified infected individuals to curb the spread. Therefore, in the absence of the ability to identify symptomatic individuals, optimal policy may only allow society to reach a level of welfare significantly below that possible in a world wherein symptomatic individuals are identified, because the social planner is unable to mandate lockdown on a comparatively small subset of the population who are symptomatic in order to realize welfare gains for the far greater share of susceptible individuals. In other words, acquiring more information can be hugely beneficial for the social welfare.

Following the calibration for the VSL, we can also examine the tradeoffs the social planner makes in lockdown, death, and hospitalization costs (Table 5). As expected, the social planner shifts costs of death and hospitalization to costs of lockdown. In particular, better information allows the social planner to lower lockdown costs dramatically. For example, being able to identify and target lockdowns on susceptible individuals so that only asymptomatic individuals are unidentified allows the social planner to mandate a much higher social activity level (at 0.70-0.85, compared to 0.57-0.62) due to the possibility of isolating symptomatic individuals. This confers a 70.4% reduction in lockdown costs, compared to a 40.7% reduction in costs of death. Intuitively, the ability for the social planner to identify symptomatic individuals lowers the costs of controlling the pandemic's trajectory such that the reproduction number does not go above 1 and that infection rates are held to a reasonable level. This is through imposing lockdown on symptomatic individuals separately so as to minimize the lockdown impact on susceptible individuals, which constitute, by far, the majority of the population.

A surprising result is the relationship between the information set of the social planner, asymptomatic rates, and the optimal policy. We would naturally assume that an optimal targeted policy would limit contacts for the older population while maintaining high social activity for the young. That is indeed the predictions of the model when the information set of the social planner implies that she cannot differentiate between susceptible and symptomatic individuals. However, if she could, the heterogeneity of asymptomatic rates will play an outsized role for the optimal policy. Since asymptomatic rates increase as age decreases, when the social planner cannot differentiate between susceptible and asymptomatic individuals, but can for other types of infected individuals, it becomes proportionately more hazardous to allow a non-symptomatic young person to socially interact, compared to that of a non-symptomatic old person. The effect of this risk may outweigh the disutility from the increased likelihood of costly infection outcomes within older people, particularly since older people are a smaller share of the population. The combination of these factors lead to

Information Set	Lockdown	Death	Hospitalization	Total Costs
$a_S = a_{I_A}, a_{I_S}, a_{I_H}$	\$1,755.1	\$236.38	\$0.207	\$1,991.7
$a_S = a_{I_A} = a_{I_S}, a_{I_H}$	\$5,948.5	\$393.09	\$0.351	\$6,341.7
$a_S = a_{I_A} = a_{I_S} = a_{I_H}$	\$7,102.6	\$469.77	\$0.430	\$7,572.8
$a_S = a_{I_A}, a_{I_S}, a_{I_H}$, homogeneous	\$1,841.4	\$248.32	\$0.221	\$2,089.9
$a_S = a_{I_A} = a_{I_S}, a_{I_H}$, homogeneous	\$6,156.7	\$404.68	\$0.362	\$6,561.7
$a_S = a_{I_A} = a_{I_S} = a_{I_H}$, homogeneous	\$7,584.8	\$496.19	\$0.438	\$8,081.4
Laissez-faire	\$3,526.0	\$10,390	\$13.0	\$13,929.0
Basic SIRD model	\$0	\$34,192	\$30.6	\$34,222.6

Table 5
Costs for different information sets

the reversal as seen in Figure 8, where the social planner seemingly paradoxically allow older people to have more social activity than younger people (dashed lines). This suggests that an optimal targeted lockdown policy may also need to factor in asymptomatic rates, though it need not be as extreme as a reversal. For example, targeted public awareness campaigns directed at the younger population encouraging vigilant self-isolating behavior even in the absence of symptomatic infection can aid in lowering the expected negative externalities.

3.6 Testing

3.6.1 Calibration

One method that the social planner may use to acquire information is testing. In order to evaluate the impact of costs of testing on optimal policy, I use different values of χ as the daily cost of testing an individual, starting with $\chi = \$127/123$[14], representing a daily testing regime with a \$127 test. Note that this implicitly assumes perfect testing. Note that the model can implicitly factor in indirect costs of testing in χ, such as the time cost of testing, within χ itself.

[14]I use the median of tests in this report(*COVID-19 Test Prices and Payment Policy*, n.d.) as the calibration.

Information Set	Lockdown	Death	Hospital	Testing	Total
Testing ($0.43)	$1.550	$33.93	$0.029	$156.60	$192.1
Testing ($5)	$55.10	$56.90	$0.049	$1,617.1	$1,729.1
Testing ($20)	$5,948.5	$393.09	$0.351	$0	$6,341.7
Testing ($127)	$5,948.5	$393.09	$0.351	$0	$6,341.7
No Testing	$5,948.5	$393.09	$0.351	$0	$6,341.7
Basic SIRD model	$0	$34,192	$30.6	$0	$34,222.6

Table 6
Costs of the pandemic with and without testing for the information set $a_S = a_{I_A} = a_{I_S}$ (perfect testing changes the information set to $a_S, a_{I_A} = a_{I_S}$).

3.6.2 Numerical Results

With $\chi = \$127/123$ or $\$20/123$, the social planner does not perform any form of testing for the given calibration. It is instructive to examine the costs of testing for the value of $\chi = \$127/123$. Suppose that the social planner chooses $\zeta = 0.1$, then the total cost of testing is

$$\int_0^\infty e^{-(\rho+\delta)t} 0.1 \cdot \frac{127}{123}\, dt = 52.343,$$

which is greater than the loss in welfare of 51.577 in Table 4 for the social planner with information set constraint $a_S = a_{I_A} = a_{I_S}$. This implies that even testing 10% of the non-hospitalized population with a $127 test daily, or to approximately test 100% of the non-hospitalized population with that test every 10 days is far too expensive. The solution to the social planner's problem with testing then degenerates to the same solution as in the previous section for the the aforementioned information set, with $\zeta(t) = 0$ for all t. Testing in this situation is not optimal because the costs of testing are far too great. Intuitively, the likelihood of identifying an infected individual is too small as the infection rate is lower than 0.1% across the population. In order to lower the negative externality by quarantining an identified infected individual, the social planner is required to use disproportionately more tests to achieve that, making persistent social distancing cheaper overall.

I find that within the model, given the initial conditions, it takes a low cost for testing to be persistently and universally utilized by the social planner. For a testing cost of $0.43,

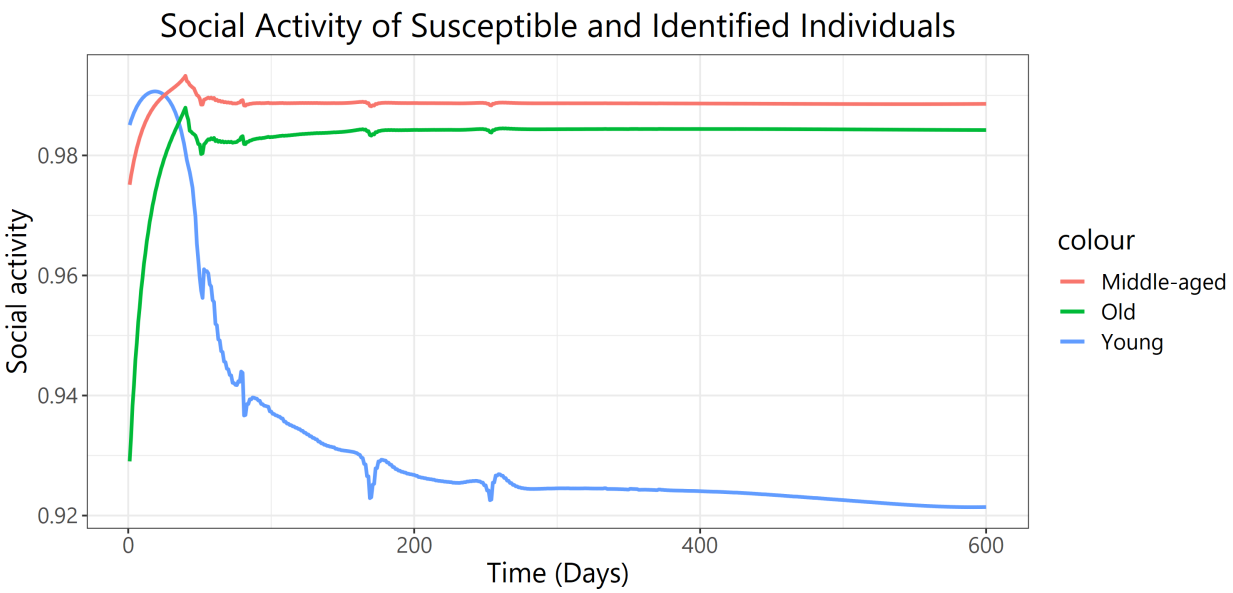

Note: The social planner chooses the minimum social activity level for identified individuals.

Figure 12
Social activity in a regime with testing for a $5 test.

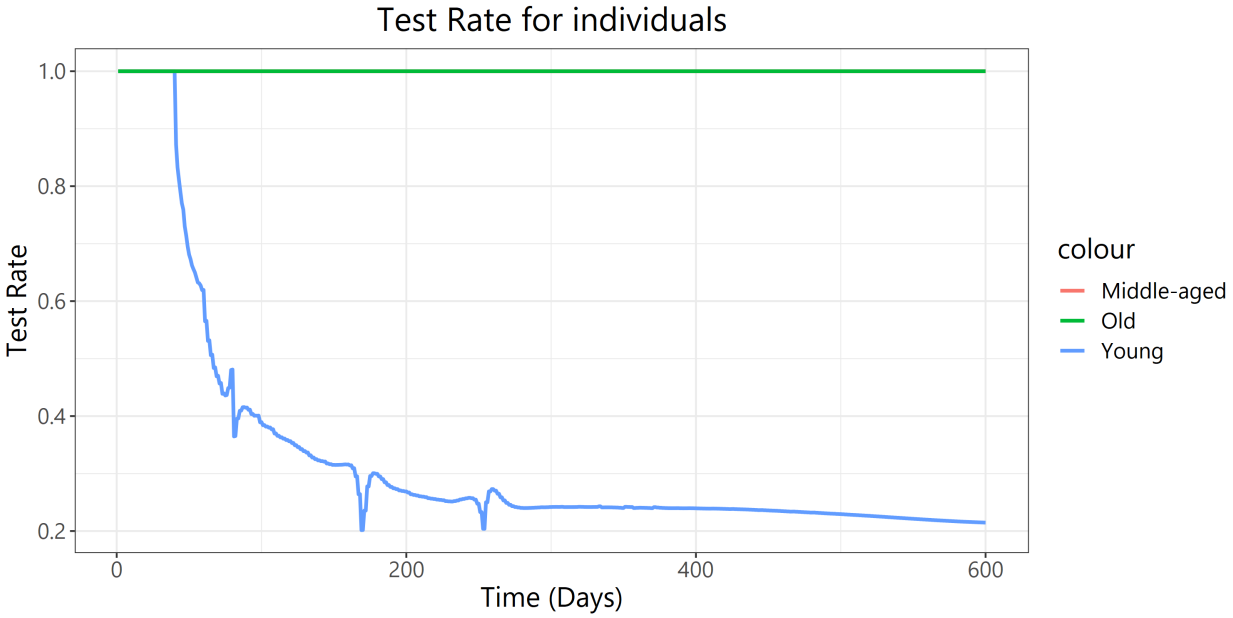

Figure 13
Testing rate for a $5 test.

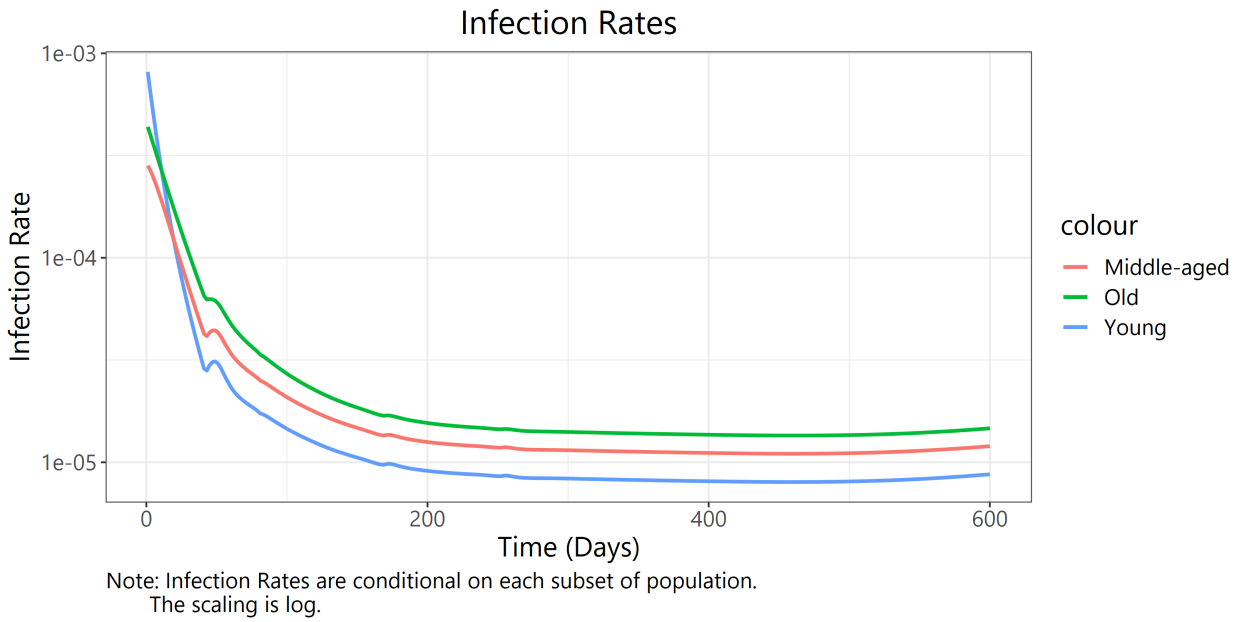

Figure 14
Infection rate for a scenario with a $5 test.

we see that the social planner does utilize daily testing at $\zeta(t) = 1$ as a policy tool for all age groups. Such a low cost of testing allows the social planner to shift costs of lockdown to costs of testing (Table 6). In this scenario, the social planner allows all susceptible individuals to have a social activity level of 1, minimizing the costs of lockdown, which are primarily the costs of quarantine by individuals who are infected. With a $5 test, however, the social planner does not utilize daily testing on all age groups. Testing rate for the middle-aged and old population is 1, but testing rate for the young population rapidly decreases over time (Figure 13). However, the optimal level of social activity still increases (Figure 12) in this scenario, once again shifting costs of lockdown to costs of testing. The rapidly decreasing testing rate on the younger population represents two effects. First, as the younger population contains the most infections at the beginning of the pandemic (Figure 9), it is optimal for the social planner to identify the infectious and quickly quarantine them from the population. Therefore, the testing rate on the young population starts at 1 at the beginning of the pandemic. However, as infections within the younger population subsides, it quickly becomes non-optimal to test the young population as heavily, because of

the young population's fast recovery rate. Therefore, infections within the young population drops faster than that of the other age groups, making it disproportionately more inefficient to identify an infected young person per test, rendering testing the young non-optimal. Instead, persistent mild lockdown on the younger population becomes more optimal than testing.

3.7 Homophily

To examine the effects of homophily I use the following association matrix representing the contact rate between susceptible individuals of each group with infected individuals of each group.

$$\begin{bmatrix} \sigma^{y,y} & \sigma^{y,m} & \sigma^{y,o} \\ \sigma^{m,y} & \sigma^{m,m} & \sigma^{m,o} \\ \sigma^{o,y} & \sigma^{o,m} & \sigma^{o,o} \end{bmatrix} = \begin{bmatrix} \alpha & 1 & 2-\alpha \\ 1 & 1 & 1 \\ 2-\alpha & 1 & \alpha \end{bmatrix}$$

with the additional association matrix

$$\begin{bmatrix} \sigma_H^{y,y} & \sigma_H^{y,m} & \sigma_H^{y,o} \\ \sigma_H^{m,y} & \sigma_H^{m,m} & \sigma_H^{m,o} \\ \sigma_H^{o,y} & \sigma_H^{o,m} & \sigma_H^{o,o} \end{bmatrix} = \begin{bmatrix} 0.7 & 0.7 & 0.7 \\ 0.7 & 0.7 & 0.7 \\ 0.6 & 0.6 & 0.6 \end{bmatrix}$$

As there is a lack of data on the true association level between groups of individuals[15], I choose these values to illustrate the qualitative behavior of the model when homophily is under consideration. I assume that young people and old people do not frequently associate and set their association to 0.6. Middle-aged adults are likely to come into contact with people of different age groups at a relatively equal weighting, owing to their statuses as parents, workers, and children of older people. I assume young people and old people have

[15]See (Ellison, 2020) for a discussion on the difficulty in calibrating association and homophily. In particular, I find that many measures of association rates capture endogenous effects that are modeled by the contact function C instead, which therefore does not map onto the model's interpretation of homophily nicely. As a result I only use values of homophily to illustrate how homophily may impact optimal policy qualitatively.

Information Set	**Welfare**	**Cumulative Deaths at Day 600**
$a_S = a_{I_A}, a_{I_S}, a_{I_H}$, $\alpha = 1$	-16.192	7.536×10^{-5}
$a_S = a_{I_A} = a_{I_S}, a_{I_H}$, $\alpha = 1$	-51.559	1.294×10^{-4}
$a_S = a_{I_A}, a_{I_S}, a_{I_H}$, $\alpha = 1.4$	-17.024	7.567×10^{-5}
$a_S = a_{I_A} = a_{I_S}, a_{I_H}$, $\alpha = 1.4$	-52.025	1.320×10^{-4}
Basic SIRD model	-308.816	0.00971

Table 7
Welfare and cumulative deaths for different information sets and homophily

Information Set	**Lockdown**	**Death**	**Hospitalization**	**Total Costs**
$a_S = a_{I_A}, a_{I_S}, a_{I_H}$, $\alpha = 1$	\$1,773.3	\$219.10	\$0.192	\$1,992.6
$a_S = a_{I_A} = a_{I_S}, a_{I_H}$, $\alpha = 1$	\$5,994.0	\$369.25	\$0.312	\$6,363.6
$a_S = a_{I_A}, a_{I_S}, a_{I_H}$, $\alpha = 1.4$	\$1,937.0	\$156.82	\$0.136	\$2,094.0
$a_S = a_{I_A} = a_{I_S}, a_{I_H}$, $\alpha = 1.4$	\$6,096.5	\$302.33	\$0.267	\$6,399.1
Basic SIRD model	\$0	\$34,192	\$30.6	\$34,222.6

Table 8
Costs for different information sets and homophily

more contact within their own groups. Finally, for hospitalized individuals, I assume that care primarily comes from hospital workers which have a median age of 45 years, and therefore set the association between hospitalized individuals and young and middle-aged individuals to 0.7, and 0.6 for older individuals. I investigate optimal policy under values of $\alpha = 1$ and 1.4.

A homophilic matching dynamic alters outcomes as shown in Tables 7 and 8. We see that homophilia induces the social planner to transfer costs of deaths to costs of lockdown in a way that increases the overall costs. Specifically, homophilic matching makes it optimal to increase the social activity of the old population, as the likelihood of infection due to increasing social activity is reduced as it is more unlikely to interact with a young individual, who are most likely to be asymptomatic. In contrast, it is more dangerous to allow a young individual to increase their social activity under homophilia as it is more difficult to lower the infection rate among younger individuals. This is because as young individuals tend to interact with young individuals, the high initial stock of infections among the young becomes harder to suppress, leading the social planner to impose a higher lockdown on those young

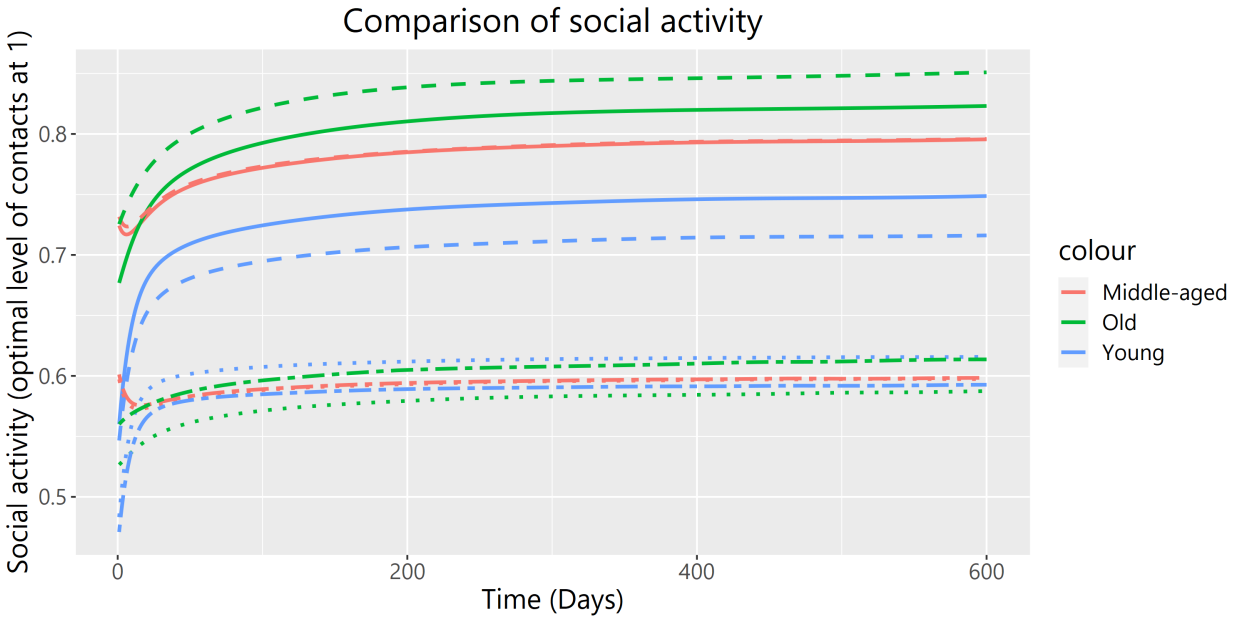

Figure 15

Social activity level for susceptible and non-identified infected individuals. The solid line corresponds to the social optimum with no homophilia and the information set $a_S = a_{I_A}, a_{I_S}, a_{I_H}$. The dashed line corresponds to the social optimum with homophilia and the same information set. The dotted line corresponds to the social optimum with no homophilia for the information set $a_S = a_{I_A} = a_{I_S}, a_{I_H}$. The dot-dash line corresponds to the same information set with homophilia. Identified infected individuals have a social activity level of $\bar{a}$, the minimal enforcement, under social optimum.

individuals.

We can then interpret this to mean that homophilia increases the sensitivity of optimal policy with respect to where the initial stock of infections are. For example, if young people tend to congregate at a town A and older people tend to congregate at a town B, if the majority of the initial stock of infections are in town A, then optimal policy will target lockdown on young people more than that if both young and older people mixed equally in both towns. Optimal policy would therefore also target lockdown on groups with a higher level of initial stock of infections.

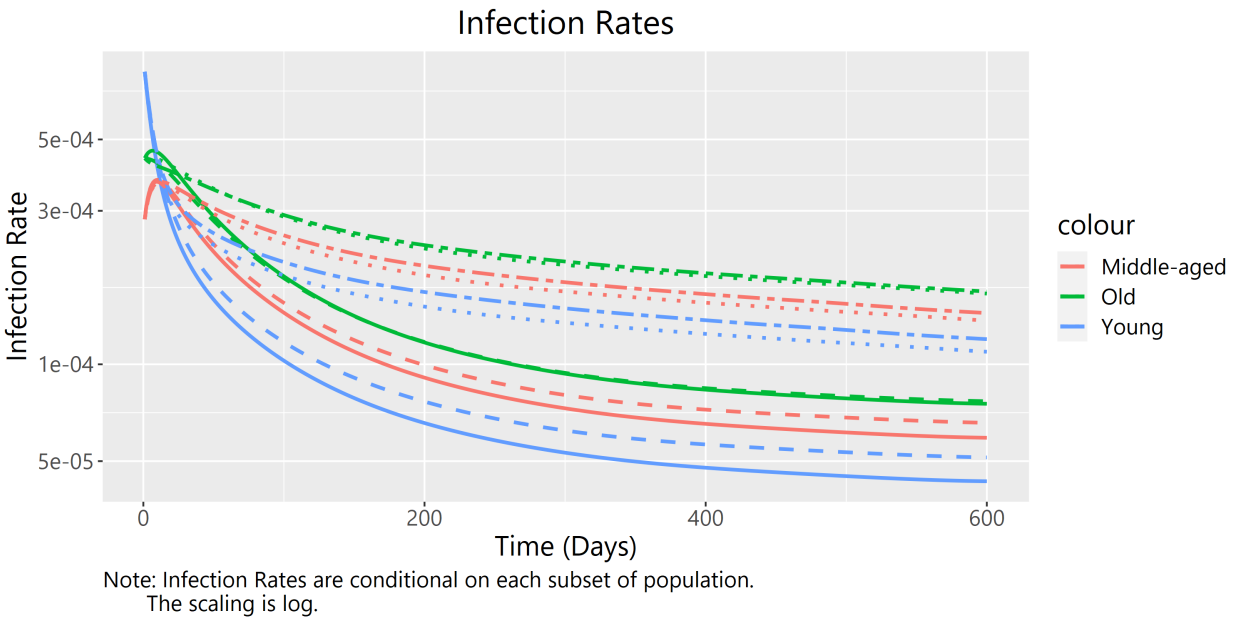

Figure 16
Infections with and without homophilic matching. The line types correspond to the same as in Figure 15.

Information Set	**Welfare**	**Cumulative Deaths at Day 600**
$a_S = a_{I_A}, a_{I_S}, a_{I_H}, \bar{a} = 0.1554$	-16.390	6.960×10^{-5}
$a_S = a_{I_A} = a_{I_S}, a_{I_H}, \bar{a} = 0.1554$	-51.886	0.000114
$a_S = a_{I_A}, a_{I_S}, a_{I_H}, \bar{a} = 0.45$	-47.521	0.000136
$a_S = a_{I_A} = a_{I_S}, a_{I_H}, \bar{a} = 0.45$	-58.194	0.000135

Table 9
Welfare and cumulative deaths for different information sets and minimum enforcement

Information Set	**Lockdown**	**Death**	**Hospitalization**	**Total Costs**
$a_S = a_{I_A}, a_{I_S}, a_{I_H}, \bar{a} = 0.1554$	\$1,773.3	\$219.10	\$0.192	\$1,992.6
$a_S = a_{I_A} = a_{I_S}, a_{I_H}, \bar{a} = 0.1554$	\$5,994.0	\$369.25	\$0.312	\$6,363.6
$a_S = a_{I_A}, a_{I_S}, a_{I_H}, \bar{a} = 0.45$	\$5,324.1	\$520.49	\$0.467	\$5,845.1
$a_S = a_{I_A} = a_{I_S}, a_{I_H}, \bar{a} = 0.45$	\$6,706.1	\$430.01	\$0.366	\$7,136.5
Basic SIRD model	\$0	\$34,192	\$30.6	\$34,222.6

Table 10
Costs for different information sets and minimum enforcement

Information Set	Lockdown	Death	Hospital	Testing	Total
Testing ($0.43)	$127.5	$104.91	$0.090	$164.3	$396.7
Testing ($5)	$6,706.1	$430.01	$0.366	$0	$7,136.5
Testing ($20)	$6,706.1	$430.01	$0.366	$0	$7,136.5
Testing ($127)	$6,706.1	$430.01	$0.366	$0	$7,136.5
No Testing	$6,706.1	$430.01	$0.366	$0	$7,136.5
Basic SIRD model	$0	$34,192	$30.6	$0	$34,222.6

Table 11
Costs of the pandemic with and without testing for the information set $a_S = a_{I_A} = a_{I_S}$ and minimum enforcement is 0.45.

3.8 Minimal Enforcement

I now turn to examine the effects of minimal enforcement on optimal policy. That welfare is substantially lower and costs higher as minimal enforcement goes up should not be surprising. However, the convergence in welfare, death, and cost outcomes between information sets as minimum enforcement goes up suggests the relative lack of benefit of testing when the social planner is unable to quarantine identified infections as effectively: as the gap between the optimal level of social activity prescribed to unidentified individuals (susceptible or asymptomatic/symptomatic) and identified individuals closes due to a lower ability to lockdown, the benefit of each unit test goes down tremendously. Indeed, from Table 11, we see that a testing cost of $5 renders testing suboptimal to persistent lockdown when $\bar{a} = 0.45$, as opposed to it being optimal when $\bar{a} = 0.1554$.

This highlights the importance of the strength of quarantine measures that can be instituted by a government. If it is mandatory for individuals identified as infected to be quarantined for weeks, as is implemented in countries like Singapore, then it is likely that widespread surveillance testing will be optimal at a higher cost, because the expected reduction in disease transmission is significant. However, if the government is unable to institute such measures due to constitutional restraints, for instance, then the benefits of widespread surveillance testing may be limited unless the cost of testing is very low.

4 Data

In this section I examine international and US national data from the COVID-19 pandemic and put the results of my model in context of these data[16]. Note that the numerical results in Section 3 are calibrated for the US, so I primarily compare qualitative findings in the model and in real world data. I detail any computational method used in Section A.

4.1 Heterogeneity in Age

I first examine the average trajectory of the pandemic for countries with more than 1 million population[17], binned by the proportion of individuals aged 65 or older and adjusted such that the first day in which the expected share of infections within the population hits 0.1%, inferred from the number of reported fatalities, is used as day 1 in the charting of the trajectory. Countries with an inferred expected share of infections that never breaks above 0.1% are dropped. I stress that the average trajectory is illustrated to get only a qualitative idea of the correlation between age and the dynamics of the pandemic (Levin et al., 2020).

From Figures 17 and 18, we can surmise two observations. The first is that countries with a greater share of old population tend to have higher peaks in new cases. This may suggest that older people are more likely to get infected per social contact, and it could also suggest that older people are more likely to be identified as infected, given their lower asymptomatic rates. The second is that deaths are higher in countries with a higher share of old individuals, which should not be surprising. The model's finding that deaths are higher within the older population is in line with this empirical observation.

Data for self-reported mitigation behaviors from April to June of 2020 (Hutchins, 2020) similarly reveal heterogeneous trends in behavioral responses to the pandemic which I summarize in Table 12. The increase in suppression of social activity by age has two confounding factors. One is the widespread social distancing guidelines in force in many states in the US,

[16]I use the publicly available panel data collated by (Max Roser and Hasell, 2020).

[17]With a population of less than 1 million, there is concern that data on the pandemic in those nations may be very noisy.

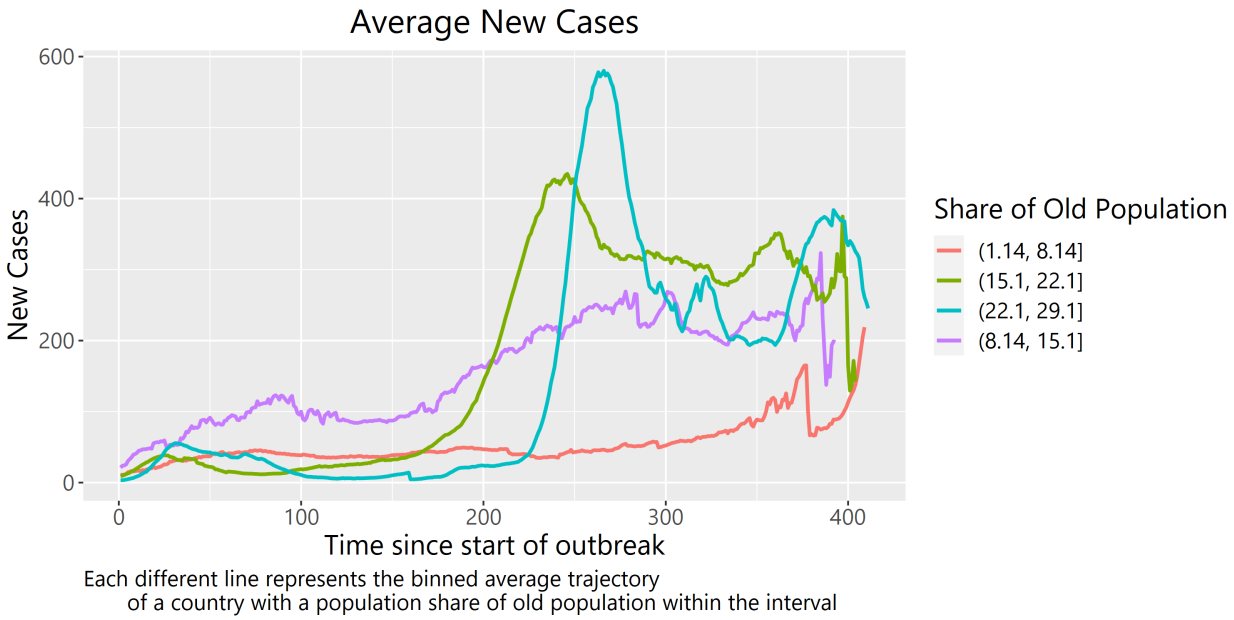

Figure 17
New cases trajectory for countries with different share of old population (per million capita)

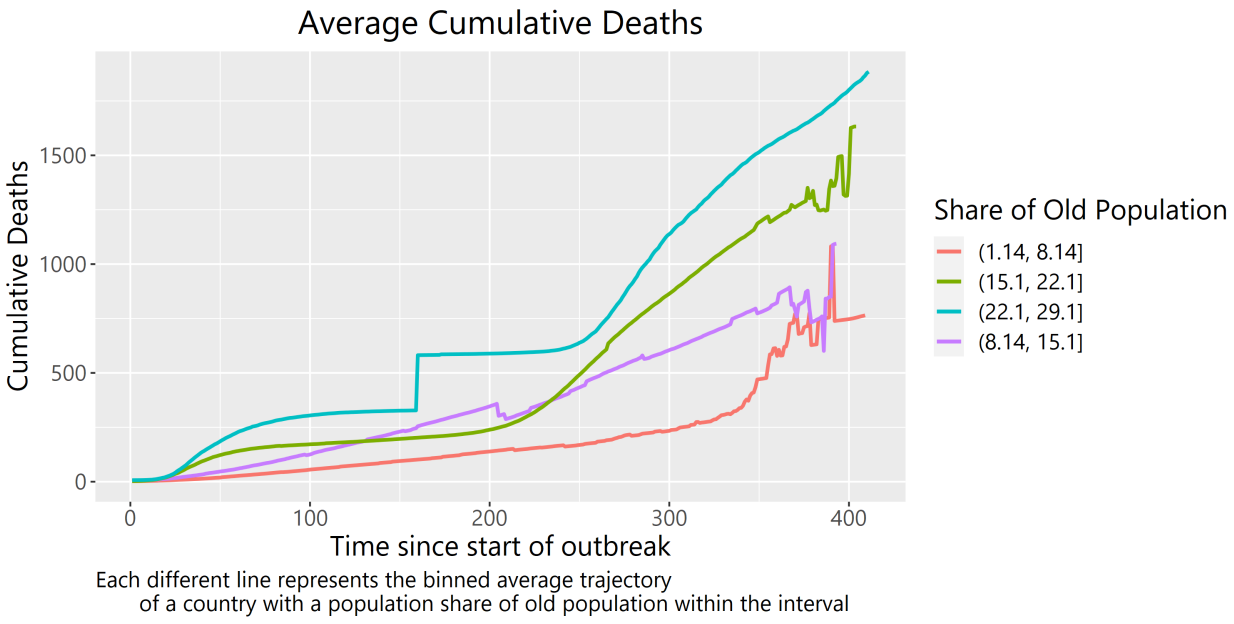

Figure 18
Cumulative deaths trajectory for countries with different share of old population (per million capita)

and the other is the self-interested behavioral response towards the illness and death heterogeneity latent within the virus. Given the lack of a nation-wide contact tracing and testing effort during this time, optimal policy would probably conform to the constraints in the information setting where infected individuals (except hospitalized) are not easily identified. In this case, both optimal policy in this information setting and laissez-faire would imply that old people pursue a lower level of social activity as the expected disutility from increasing their contact is relatively higher. However, as the US's social distancing and lockdown guidelines during this period are largely non-targeted, the heterogeneity in the behavioral data across age is more likely due to laissez-faire optimization. That an imperfectly enforced universal policy can nevertheless result in heterogeneous behaviors qualitatively similar to a perfectly enforced targeted policy illustrates that it is possible that a well-designed universal policy may induce a close-to-optimal heterogeneous behavioral outcome in the face of a pandemic. This can be beneficial as in general it may be unpopular or difficult to implement a targeted lockdown policy.

However, it is also possible that such behavior is unwanted. If it is possible to identify and lockdown symptomatic individuals, optimal policy may dictate that the younger population sacrifice equal, if not more, social activity as the older population, as we have seen in the numerical examples (Figure 8). In this case, leaving the younger population to optimize under a universal policy may be sub-optimal as it is likely they would not internalize the relatively larger externality due to their much higher likelihood of being asymptomatically infectious, maintaining a higher level of social activity than in the optimal policy. This increases the costs of hospitalization and deaths and also the cost of self-isolation more broadly. The lack of negative externality internalizing on the part of the younger population will force middle-aged and older people to self-isolate more heavily than they need to under optimal policy in this information setting.

Age Group	Canceled social activities	Avoided crowded places	Avoided restaurants
18-29	61.3%	71.9%	64.5%
30-44	65.4%	74.8%	69.2%
45-59	67.5%	77.7%	69.7%
≥ 60	70.6%	83.0%	75.4%

Table 12
Heterogeneity in social activity by age group

4.2 Testing

To examine testing, I use US county-level data from the CMS and JHU[18] on testing and health outcomes from September 2020 to April 2021 to investigate the relationship between the two and run the simple panel model

$$d_{it} = \alpha x_{i(t-5)} + \beta c_{i(t-2)} + \gamma \mathbf{v_{it}} + s_i + w_t + \epsilon_{it} \tag{25}$$

where d_{it} is the death rate of county i in period t, x_{it} is the test rate, c_{it} is the case infection rate, $\mathbf{v_{it}}$ are additional controls, s_i and w_t are fixed effects for county and for seasonality. The death rate of COVID-19 is affected by the effective infection fatality ratio and the number of infections leading up to the death. The case infection rate from 2 weeks prior captures the latter effect, conditional on the assumption that the proportion of cases in each severity category stays relatively stable throughout the panel's timeframe. The effective infection fatality ratio is affected by differences in demographics, healthcare infrastructure, and policies, captured by the county fixed effects. Additional controls include ICU capacity. This limits the possible biased contribution of unobserved variables, although I stress that in the absence of more granular data on more possibly unobserved variables on the pandemic the results should only be treated as an initial suggestion.

The results in Table 13 suggests that prior test rate and death rate may be negatively correlated. The possible mechanism for this correlation may be the information revealing

[18]https://data.cms.gov/stories/s/q5r5-gjyu, (*COVID-19 Nursing Home Data*, n.d.) and (Dong et al., 2020)

Table 13
Correlation between Death Rate and Test Rate at the County Level

	Dependent variable:
	Death Rate
Test Rate (1 month Prior)	−0.034
	(−0.037, −0.031)
	p = 0.000***
Positivity Rate (2-4 weeks Prior)	−0.010
	(−0.011, −0.010)
	p = 0.000***
Constant	0.010
	(0.010, 0.011)
	p = 0.000***
County Fixed Effects	Yes
Seasonality Effects	Yes
Observations	21,768
R^2	0.071
Adjusted R^2	0.071
F Statistic	1,655.894***
Note:	*p<0.1; **p<0.05; ***p<0.01

mechanism associated with testing. As testing reveals mildly symptomatic and asymptomatic individuals' true infection status, policymakers and individual altruism may adjust individual behaviors so as to limit infection spread more effectively. This in turn leads to lower deaths. This corresponds to the prediction of the model that testing reduces the amount of deaths. I argue that such an adjustment, however, may have limited benefits. When the stock of infection is relatively low, the expected benefit from testing is also low, which may lead to policymakers and individuals suppressing social activity as it may have relatively higher value than testing. In other words, to limit the costs of death from infections by lowering infections, testing may be a more expensive route than social distancing and lockdowns.

5 Discussion

Heterogeneity and information are intrinsically linked in an optimal policy during a pandemic. As the COVID-19 pandemic affects different groups of people differently, especially by age, it can be optimal to institute a targeted policy by age instead of a universal policy. However, the degree to which an optimal targeted policy by age is superior to a universal policy also depends on the level of information a social planner has. For example, one source of heterogeneity by age in the COVID-19 pandemic is the high variance in symptomatic rates by age. If a social planner is able to identify asymptomatic individuals, for example, then a targeted policy may only be marginally more beneficial than a universal policy as the social planner can use lockdown on asymptomatic individuals as a proxy measure for lockdown on young individuals, as young individuals are most likely to be asymptomatic. Hence, identification of infection states of individuals and targeted lockdown measures are weak substitutes of each other. Although this paper examined one facet of heterogeneity - symptomatic and hospitalization rates by age - identification on the infection statuses across other variances, such as essential workers versus non-essential workers, individuals who may

work from home easily versus those who cannot, can be hugely beneficial in a targeted policy.

The trade off between acquiring more information on the state of the pandemic and persistent lockdown and social distancing depends on several factors. First, costs of information acquisition, such as testing and contact tracing, need to be sufficiently low for information acquisition to be optimal. I stress that this paper examined a form of testing that is largely random and best matches widespread surveillance testing so cannot evaluate the optimality of other types of testing, such as contact tracing, which is network-based instead of random. Intuitively, widespread surveillance testing is optimal when the stock of infections and the ability to apply high levels of lockdown are relatively large as they increase the expected benefit from each unit of test. Contact tracing on the other hand may be more optimal when the stock of infections is low as the expected probability of identifying an infectious person is relatively larger than that of widespread random testing in this case. In the US, many contact tracing programs have shown limited efficacy possibly because the costs of contact-tracing based interventions are far too high when the stock of infections is large. In this case, it may be beneficial for such states to temporarily switch to a widespread and cheap testing program to lower the infection rates instead. On the other hand, the success of the contact tracing program in Taiwan may reflect the relative lower costs of contact tracing when the stock of infections is low. Hence, it is possible that a balance of untargeted testing and network-targeted testing is needed, depending on the state of the pandemic and the demographics.

Finally, the social planner in this model is utilitarian, and weighs the utility derived from social activity for each individual equally. In general, it is possible to argue for different Pareto optimal outcomes. For example, the depreciation in human capital from extended lockdown may be heterogeneous across individuals. Younger individuals may be disproportionately impacted by lockdown and society may also wish to prioritize certain groups of individuals to be relieved of lockdown over others. Specifically, a value system that emphasizes in-person education and training for younger individuals may choose a social optimum

that imposes lower social activity for older and middle-aged individuals and a higher social activity for younger individuals. Hence, the utilitarian social optimum should be treated as a starting point rather than an endpoint.

5.1 Conclusion

In this paper I examined a heterogeneous SIRD model with endogenous social activity and examined optimal policy under various conditions. Optimal policy would likely entail some level of targeting, but the information structure that a government is facing can also influence that optimal policy. For example, different levels of asymptomatic rates in different subgroups of the population can dramatically change the optimal policy, indicating that the level of information a social planner has can interact with underlying heterogeneity in the population. Policies that impact the information structure, such as testing, can generate welfare gains if the costs of acquiring more information is sufficiently low. Investment into programs that could improve the clarity and precision of information that a government is working with can be beneficial for future pandemics.

References

Acemoglu, Daron, Victor Chernozhukov, Iván Werning, and Michael D. Whinston, "Optimal Targeted Lockdowns in a Multi-Group SIR Model," Technical Report w27102, National Bureau of Economic Research May 2020.

Almagor, Jonatan and Stefano Picascia, "Exploring the effectiveness of a COVID-19 contact tracing app using an agent-based model," *Scientific Reports*, December 2020, *10* (1), 22235.

Alvarez, Fernando E., David Argente, and Francesco Lippi, "A Simple Planning Problem for COVID-19 Lockdown," Technical Report w26981, National Bureau of Economic Research April 2020.

Arias, Jonas E, Jesús Fernández-Villaverde, Juan Rubio Ramírez, and Minchul Shin, "Bayesian Estimation of Epidemiological Models: Methods, Causality, and Policy Trade-Offs," Working Paper 28617, National Bureau of Economic Research March 2021.

Atkeson, Andrew, Karen A. Kopecky, and Tao Zha, "Behavior and the Transmission of COVID-19," Technical Report 618, Federal Reserve Bank of Minneapolis February 2021.

Ayres, Ian, Alessandro Romano, and Chiara Sotis, "How to Make COVID-19 Contact Tracing Apps Work: Insights From Behavioral Economics," SSRN Scholarly Paper ID 3689805, Social Science Research Network, Rochester, NY September 2020.

Bartsch, Sarah M., Marie C. Ferguson, James A. McKinnell, Kelly J. O'Shea, Patrick T. Wedlock, Sheryl S. Siegmund, and Bruce Y. Lee, "The Potential Health Care Costs And Resource Use Associated With COVID-19 In The United States," *Health Affairs*, April 2020, *39* (6), 927–935.

Broyden, C. G., "The Convergence of a Class of Double-rank Minimization Algorithms 1. General Considerations," *IMA Journal of Applied Mathematics*, March 1970, *6* (1), 76–90.

Bureau, US Census, "National Demographic Analysis Tables: 2020."

Calgary, Open, "Provisional COVID-19 Death Counts by Sex, Age, and State | Data | Centers for Disease Control and Prevention."

CDC, "Healthcare Workers," February 2020.

Cevik, Muge, Matthew Tate, Ollie Lloyd, Alberto Enrico Maraolo, Jenna Schafers, and Antonia Ho, "SARS-CoV-2, SARS-CoV, and MERS-CoV viral load dynamics, duration of viral shedding, and infectiousness: a systematic review and meta-analysis," *The Lancet Microbe*, January 2021, *2* (1), e13–e22.

Cori, Anne, Neil M. Ferguson, Christophe Fraser, and Simon Cauchemez, "A New Framework and Software to Estimate Time-Varying Reproduction Numbers During Epidemics," *American Journal of Epidemiology*, November 2013, *178* (9), 1505–1512.
COVID-19 Nursing Home Data

COVID-19 Nursing Home Data.
COVID-19 Test Prices and Payment Policy

COVID-19 Test Prices and Payment Policy.

Crane, Matthew A., Kenneth M. Shermock, Saad B. Omer, and John A. Romley, "Change in Reported Adherence to Nonpharmaceutical Interventions During the COVID-19 Pandemic, April-November 2020," *JAMA*, 03 2021, *325* (9), 883–885.

Davies, Nicholas G., Petra Klepac, Yang Liu, Kiesha Prem, Mark Jit, and Rosalind M. Eggo, "Age-dependent effects in the transmission and control of COVID-19 epidemics," *Nature Medicine*, August 2020, *26* (8), 1205–1211.

dinoverm, "Density-dependent vs. Frequency-dependent Disease Transmission," October 2013.

Dong, Ensheng, Hongru Du, and Lauren Gardner, "An interactive web-based dashboard to track COVID-19 in real time," *The Lancet Infectious Diseases*, May 2020, *20* (5), 533–534.

Eichenbaum, Martin S., Sergio Rebelo, and Mathias Trabandt, "The Macroeconomics of Epidemics," Technical Report w26882, National Bureau of Economic Research March 2020.

Ellison, Glenn, "Implications of Heterogeneous SIR Models for Analyses of COVID-19," Technical Report w27373, National Bureau of Economic Research June 2020.

Farboodi, Maryam, Gregor Jarosch, and Robert Shimer, "Internal and External Effects of Social Distancing in a Pandemic," Working Paper 27059, National Bureau of Economic Research April 2020.

Farhi, Michael J. Mina and James David Baqaee Stock Emmanuel, "Policies for a second wave," June 2020.

Fenichel, Eli P., "Economic considerations for social distancing and behavioral based policies during an epidemic," *Journal of Health Economics*, March 2013, *32* (2), 440–451.

_ , Carlos Castillo-Chavez, M. G. Ceddia, Gerardo Chowell, Paula A. Gonzalez Parra, Graham J. Hickling, Garth Holloway, Richard Horan, Benjamin Morin, Charles Perrings, Michael Springborn, Leticia Velazquez, and Cristina Villalobos, "Adaptive human behavior in epidemiological models," *Proceedings of the National Academy of Sciences*, April 2011, *108* (15), 6306–6311.

Ferguson, N, D Laydon, G Nedjati Gilani, N Imai, K Ainslie, M Baguelin, S Bhatia, A Boonyasiri, ZULMA Cucunuba Perez, G Cuomo-Dannenburg, A Dighe, I Dorigatti, H Fu, K Gaythorpe, W Green, A Hamlet, W Hinsley, L Okell, S Van Elsland, H Thompson, R Verity, E Volz, H Wang, Y Wang, P Walker, P Winskill, C Whittaker, C Donnelly, S Riley, and A Ghani, "Report 9: Impact of non-pharmaceutical interventions (NPIs) to reduce COVID19 mortality and healthcare demand," Technical Report, Imperial College London March 2020.

Gao, Zhiru, Yinghui Xu, Chao Sun, Xu Wang, Ye Guo, Shi Qiu, and Kewei Ma, "A systematic review of asymptomatic infections with COVID-19," *Journal of Microbiology, Immunology and Infection*, 2021, *54* (1), 12–16.

Gostic, Katelyn M., Lauren McGough, Edward B. Baskerville, Sam Abbott, Keya Joshi, Christine Tedijanto, Rebecca Kahn, Rene Niehus, James Hay, Pablo M. De Salazar, Joel Hellewell, Sophie Meakin, James Munday, Nikos I. Bosse, Katharine Sherrat, Robin N. Thompson, Laura F. White, Jana S. Huisman, Jérémie Scire, Sebastian Bonhoeffer, Tanja Stadler, Jacco Wallinga, Sebastian Funk, Marc Lipsitch, and Sarah Cobey, "Practical considerations for measuring the effective reproductive number, Rt," *medRxiv*, August 2020.

Hall, Robert E., Charles I. Jones, and Peter J. Klenow, "Trading Off Consumption and COVID-19 Deaths," Technical Report w27340, National Bureau of Economic Research June 2020.

Hutchins, Helena J., "COVID-19 Mitigation Behaviors by Age Group — United States, April–June 2020," *MMWR. Morbidity and Mortality Weekly Report*, 2020, *69.*

Jian, Shu-Wan, Hao-Yuan Cheng, Xiang-Ting Huang, and Ding-Ping Liu, "Contact tracing with digital assistance in Taiwan's COVID-19 outbreak response," *International Journal of Infectious Diseases*, December 2020, *101*, 348–352.

Kermack, William and A. G. McKendrick, "Contributions to the mathematical theory of epidemics. II. —The problem of endemicity," *Proceedings of the Royal Society of London. Series A, Containing Papers of a Mathematical and Physical Character*, October 1932, *138* (834), 55–83.

Levin, Andrew T., William P. Hanage, Nana Owusu-Boaitey, Kensington B. Cochran, Seamus P. Walsh, and Gideon Meyerowitz-Katz, "Assessing the age specificity of infection fatality rates for COVID-19: systematic review, meta-analysis, and public policy implications," *European Journal of Epidemiology*, December 2020, *35* (12), 1123–1138.

Lopez-Leon, Sandra, Talia Wegman-Ostrosky, Carol Perelman, Rosalinda Sepulveda, Paulina A. Rebolledo, Angelica Cuapio, and Sonia Villapol, "More than 50 Long-term effects of COVID-19: a systematic review and meta-analysis," *medRxiv*, January 2021, p. 2021.01.27.21250617.

Lurie, Mark N, Joe Silva, Rachel R Yorlets, Jun Tao, and Philip A Chan, "Coronavirus Disease 2019 Epidemic Doubling Time in the United States Before and During Stay-at-Home Restrictions," *The Journal of Infectious Diseases*, October 2020, *222* (10), 1601–1606.

McCallum, Hamish, Nigel Barlow, and Jim Hone, "How should pathogen transmission be modelled?," *Trends in Ecology & Evolution*, June 2001, *16* (6), 295–300.

Nonno, Franca Del, Daniele Colombo, Roberta Nardacci, and Laura Falasca, "Fatal pulmonary arterial thrombosis in a COVID-19 patient, with asymptomatic history, occurred after swab negativization," *Thrombosis Journal*, January 2021, *19* (1), 1.

Philipson, Tomas, "Economic Epidemiology & Infectious Diseases," SSRN Scholarly Paper ID 155528, Social Science Research Network, Rochester, NY January 2000.

Ritchie, Esteban Ortiz-Ospina Max Roser Hannah and Joe Hasell, "Coronavirus Pandemic (COVID-19)," *Our World in Data*, 2020. https://ourworldindata.org/coronavirus.

Ritchie, Hannah and Max Roser, "Age Structure," *Our World in Data*, 2019. https://ourworldindata.org/age-structure.

Smith, Matthew J., Sandra Telfer, Eva R. Kallio, Sarah Burthe, Alex R. Cook, Xavier Lambin, and Michael Begon, "Host–pathogen time series data in wildlife support a transmission function between density and frequency dependence," *Proceedings of the National Academy of Sciences*, May 2009, *106* (19), 7905–7909.

Toxvaerd, Flavio, "Rational Disinhibition and Externalities in Prevention," *International Economic Review*, 2019, *60* (4), 1737–1755.
Vaccine Distribution Phases

Vaccine Distribution Phases.

Verity, Robert, Lucy C. Okell, Ilaria Dorigatti, Peter Winskill, Charles Whittaker, Natsuko Imai, Gina Cuomo-Dannenburg, Hayley Thompson, Patrick G. T. Walker, Han Fu, Amy Dighe, Jamie T. Griffin, Marc Baguelin, Sangeeta Bhatia, Adhiratha Boonyasiri, Anne Cori, Zulma Cucunubá, Rich FitzJohn, Katy Gaythorpe, Will Green, Arran Hamlet, Wes Hinsley, Daniel Laydon, Gemma Nedjati-Gilani, Steven Riley, Sabine van Elsland, Erik Volz, Haowei Wang, Yuanrong Wang, Xiaoyue Xi, Christl A. Donnelly, Azra C. Ghani, and Neil M. Ferguson, *"Estimates of the severity of coronavirus disease 2019: a model-based analysis," The Lancet Infectious Diseases, June 2020, 20 (6), 669–677.*

Wortham, Jonathan M., *"Characteristics of Persons Who Died with COVID-19 — United States, February 12–May 18, 2020," MMWR. Morbidity and Mortality Weekly Report, 2020, 69.*

Yang, Rongrong, Xien Gui, and Yong Xiong, *"Comparison of Clinical Characteristics of Patients with Asymptomatic vs Symptomatic Coronavirus Disease 2019 in Wuhan, China," JAMA Network Open, May 2020, 3 (5), e2010182.*

A Computational Method

A Model Computational Method

In this section, I describe the method to solve for the model as described in the social planner's problem as described by Equation 4, subject to the dynamic constraints Equations 1. The computational method for other extensions follow the same strategy. Due to issues with numerical accuracy and the highly unstable behavior exhibited by the equilibrium flow in the heterogeneous model rendering backward Runge-Kutta (of 8th degree) shooting methods infeasible, I instead discretized the model and solved for optimal path of social activity directly instead. Doing so necessarily implies that the numerical results are approximations to the real solution for the continuous version of the model described in this paper.

For a given discretized social activity path from time 0 to T, we can solve for the value of the objective function for the social planner directly. Hence, there is some function $f : \mathbb{R}^n \to \mathbb{R}$ for a vector $(a_0, \ldots, a_T)$ that we may optimize, which takes the social activity path as a vector and outputs the value of the objective function for the social planner. Note however that for f to approximate the social planner's objective well we require T to be sufficiently large. For this purpose I set T to 2000. I employ the limited memory Broyden–Fletcher–Goldfarb–Shanno algorithm (Broyden, (1970)) to optimize on f directly. To do so efficiently, I first optimize on a discretized model with 10-day intervals, which reduces the complexity of the optimization drastically. This gives us a discretized social activity path that we may use to initialize the optimization for the actual discretized model with an initial guess that is close to the actual optimal social activity path. Doing so reduces the time taken for the BFGS optimization algorithm by up to 5 times as measured (as opposed to a naive initial guess of $(1, \ldots, 1)$).

Furthermore, as the BFGS algorithm requires f to be differentiable, I verify f's differentiability as follows: First take any component a_x and examine the partial derivative $\partial f / \partial a_x$. Since the objective function f is a discretized sum of exponentially discounted terms that

are consistent each time period, we may simply show that the partial derivative $\partial f_t/\partial a_x$ is continuous everywhere, where f_t is the term in period t. For the term within Equation 3 we see that we may simply verify that the partial derivative of the state variables in any time period with respect to a_x is continuous, and similarly for the utility function. The latter is shown by observing that the logarithm function is differentiable. For the former, notice that the state variables are differentiable functions of state variables in the previous time period. At the time period x then, observe that a_x appears in the contact function, of which the partial derivatives are continuous. Hence, the partial derivatives of the same-period state variables with respect to a_x is continuous, and hence all subsequent state variables have continuous partial derivatives with respect to a_x as they are differentiable compositions. Hence f is differentiable since our choice of a_x was arbitrary.

It is then straightforward to compute f as follows: Given a social activity path vector, we start with the initial conditions for the state variables and compute the next period's state variables with the equivalent difference equations as in Equations 1. We can then approximate integration via summation and find an approximate value to the objective function given sufficiently large T.

The code can be found on Github[19].

B Data Computational Method

B.1 Date of Initial Outbreak

To estimate the date of initial outbreak, I make the assumption that the infection fatality ratio is exponential in age[20]. Doing so, we can estimate the average infection fatality ratio of each country based on its demographic data[21]. We can then estimate the date of initial outbreak by searching for the first time period t wherein after a weighted average of $1/\gamma_S$ and $1/\gamma_H$ days the proportion of deaths in the population divided by the infection fatality

[19]Code link: https://github.com/Skyrior/HetSIRD-econ/blob/main/thesis.R

[20]This is supported by the medical literature. For example, see (Levin et al., 2020).

[21]I use the demographic data in (Ritchie and Roser, 2019)

ratio is 0.1%.